MODELING GROUNDWATER FLOW AND CONTAMINANT TRANSPORT IN FRACTURED AQUIFERS

THESIS

Jason M. Bordas, Captain, USAF

AFIT/GEM/ENV/05M-02

DEPARTMENT OF THE AIR FORCE
AIR UNIVERSITY

AIR FORCE INSTITUTE OF TECHNOLOGY

Wright-Patterson Air Force Base, Ohio

The views expressed in this thesis are those of the author and do not reflect the official policy or position of the United States Air Force, Department of Defense, or the United States Government.

AFIT/GEM/ENV/05M-02

MODELING GROUNDWATER FLOW AND CONTAMINANT TRANSPORT IN FRACTURED AQUIFERS

THESIS

Presented to the Faculty

Department of Systems and Engineering Management

Graduate School of Engineering and Management

Air Force Institute of Technology

Air University

Air Education and Training Command

In Partial Fulfillment of the Requirements for the

Degree of Master of Science in Engineering Management

Jason M. Bordas, BS

Captain, USAF

March 2005

AFIT/GEM/ENV/05M-02

MODELING GROUNDWATER FLOW AND CONTAMINANT TRANSPORT IN FRACTURED AQUIFERS

Jason M. Bordas, BS
Captain, USAF

Approved:

/signed/	16 March 2005
Dr. Mark N. Goltz (Chairman)	date
/signed/	16 March 2005
Dr. Alfred E. Thal, Jr. (Member)	date
/signed/	16 March 2005
Dr. Junqi Huang (Member)	date

Abstract

Fractured aquifers are a valuable source of groundwater throughout the world. Fractures often serve as major conduits for movement of water and dissolved chemicals through impermeable or low permeability rock. Unfortunately, the ease with which water and chemicals are transmitted through fractures leaves fractured aquifers vulnerable to pollution from a range of industrial and agricultural activities.

Of concern to the Department of Defense (DoD) is that a number of major US military installations, such as Ramstein Air Base (AB) and Spangdahalem AB, Germany and Osan AB, Republic of Korea, are located above contaminated fractured aquifers. In addition, a number of former DoD installations, such as Pease Air Force Base (AFB), New Hampshire, and Loring AFB, Maine, are located above fractured aquifers and are contaminated to such an extent that they have been placed on the National Priority List for cleanup under the Superfund program.

This study focused on reviewing the current state-of-the-art of modeling groundwater flow and contaminant transport in fractured media. Such models can be used to aid our understanding of the physical, chemical, and biological processes that affect contaminant transport in fractured media, as well as help us design systems to remediate contaminated fractured sites. After reviewing available models, the hybrid discrete fracture network/equivalent porous medium (DFN/EPM) model was selected for further analysis. The DFN/EPM model was selected because it appeared to have the potential to aid decision making by remedial project managers at contaminated DoD fractured aquifer sites. This model can use data that are typically available at a site while incorporating the important processes relevant to describing contaminant transport in a fractured medium.

The model was applied to simulate the operation of a pump-and-treat remedial action at a trichloroethene-contaminated fractured aquifer at Pease AFB. The model was able to simulate the salient characteristics of hydraulic and contaminant data collected at the site during operation of the remediation pump-and-treat system. The model was then used to evaluate the impact of various pump-and-treat system designs on contaminant containment at the site. Based on these model simulations, the potential benefits to site managers of using the DFN/EPM approach to model groundwater flow and contaminant transport at fractured aquifer sites were demonstrated.

Acknowledgements

There are several individuals I would like to recognize for helping me complete this thesis. I would first like to extend my appreciation to Dr. Mark Goltz. His patience, guidance, and support carried me through the course of this research effort. I would also like to thank Dr. Junqi Huang for the many times I entered his office with a question about the GMS model. I also would like to thank Dr. Thal for his comments and insight which improved the final product. This study could not have been completed without the information on Pease AFB supplied by Mr. Peter Forbes of the Air Force Real Property Agency.

Thanks go to my children, whose sudden distractions offered respite from the thesis effort.

The final contributor to this effort is my wife. My heartfelt thanks go to her for all the times I was at home but she was alone. I will always remember her patience, understanding, and support.

Thank you all.

Jason M. Bordas

Table of Contents

Page

Page

List of Figures

Page

Page

Page

List of Tables

Page

MODELING GROUNDWATER FLOW AND CONTAMINANT TRANSPORT IN FRACTURED AQUIFERS

1 Introduction

1.1 Motivation

Fractured aquifers are a valuable source of groundwater throughout the world. These aquifers have the capacity to store large volumes of water and to deliver groundwater to wells through a network of fractures. Fractures often serve as major conduits for movement of water and dissolved chemicals through hard rocks in the subsurface. Unfortunately, the ease with which water and chemicals are transmitted through fractures leave fractured aquifers vulnerable to pollution from a range of industrial and agricultural activities (Wealthall *et al.*, 2003). Throughout the world, groundwater resources are faced with an unprecedented risk of contamination due to subsurface releases of organic chemicals such as chlorinated solvents and petroleum hydrocarbons. In the United States (U.S.) alone, releases of gasoline fuels may have occurred at more than 250,000 sites, potentially threatening over 9,000 large municipal water supply wells (Einarson and Mackay, 2001).

Of concern to the Department of Defense (DoD) is that a number of major US military installations, such as Ramstein Air Base (AB), Germany; Spangdahalem AB, Germany; and Osan AB, Republic of Korea; are located above contaminated fractured aquifers. In addition, a number of closed bases such as Pease Air Force Base (AFB), New Hampshire, and Loring AFB, Maine, are located above fractured aquifers and are contaminated to such an extent that they have been placed on the National Priority List

for cleanup under the Superfund program. Dissolution of pollutants in fractured aquifers can lead to dissolved plumes with contaminant concentrations that can exceed drinking water standards (Wealthall *et al.*, 2003). At Osan AB, chlorinated solvents such as trichloroethylene (TCE) have been detected in groundwater wells at concentrations of 83 μg/L; 17 times greater than its maximum concentration level (MCL) under the Safe Drinking Water Act (Osan AB CE, 2001). TCE has been found to cause vomiting and abdominal pain at levels above the MCL, and it has the potential to cause liver damage and cancer with prolonged exposure above the MCL (EPA, 2002). This is of particular concern because the wells at Osan AB are needed for surge operations should U.S. forces build up their presence on the Korean peninsula (Staples, 2002). Pease AFB has detected TCE in groundwater at concentrations of over 100 mg/L (MWH, 2004). Ramstein AB has a dissolved plume of TCE advancing through its fractured aquifer with the potential to cross the installation boundary (Ramstein AB CE, 2003). In addition, former military installations that have been closed, such as Pease and Loring AFB, require a substantial amount of cleanup before the property can be turned over for civilian use.

Over the last several decades, models have been increasingly used to aid subsurface remediation decision making. These models are based on Henri Darcy's 1857 law describing flow in porous media. Due in large part to the complexity of flow in fractured rock systems, the state-of-the-art of modeling such fractured flow has significantly lagged the state-of-the-art of modeling porous media flow (USEPA, 2002).

Driven in large part by advances in computer resources, great strides in numerical modeling of groundwater systems have been made in recent years (Hassan, 2004). With these advances in computers and our increased knowledge of flow and transport behavior

in fractured systems, attempts can now be made to deal with these more complex problems. It would be hoped that fractured flow and transport models can be developed to become practical aids to decision making in the same way that porous media models are. Having the ability to model water flow and contaminant transport in fractured aquifers would provide scientists, engineers, and decision makers involved in the assessment and remediation of groundwater pollution with a useful tool that they can use to develop containment and cleanup strategies.

1.2 Background

Fractured rock sites are among the most complex because of their considerable geologic heterogeneity and the nature of fluid flow and contaminant transport through the fractured material. Relative to most unconsolidated media, characterization of contaminant transport in fractured rock requires more information to provide a similar level of understanding (EPA, 2001). Therefore, modeling of contaminant transport within fractured rock is a significant challenge (Wealthall *et al.*, 2003). Contaminant transport in fractured rock is governed by advection, dispersion, diffusion, and biological and chemical reactions. These are the same processes that govern transport in granular media, but transport in fractured systems depends more heavily on the physical makeup of the rock matrix. Most fractured rock systems consist of solid rock mass intersected by fractures (Figure 1.1).

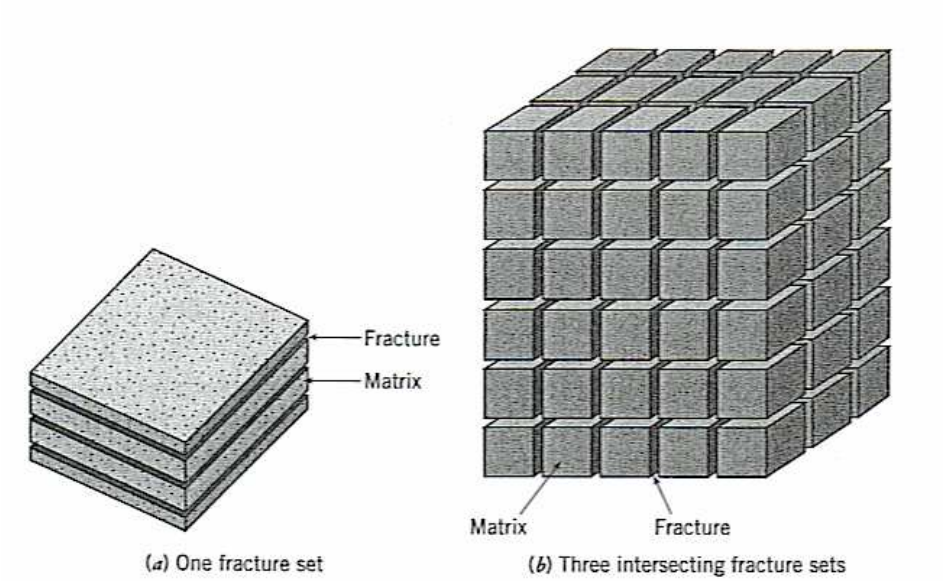

Figure 1.1: Representation of fractures within the rock matrix (From Schwartz and Zhang, 2003)

Fractures provide conduits for the movement of groundwater and contaminants through a relatively impermeable rock mass. The water in the rock matrix is assumed to be stagnant, but can act as storage for dissolved contaminants as they diffuse from the flowing fracture into the matrix blocks (EPA, 2002). For many of the same reasons that we have been motivated over the past several decades to develop confidence in our ability to model flow and chemical transport in porous media, we now need to develop confidence in our abilities to model flow and transport in fractured media.

Modeling flow and transport in fractured rocks is relatively complex because the fractures can be as difficult to observe and characterize as they are to represent in a numerical model. Alternative modeling approaches infer properties, represent fractures, and resolve scale dependencies in different ways (Selroos *et al.*, 2002). This research

will look at the current state-of-the-art of fractured flow models and choose one or more to evaluate.

Stochastic continuum modeling of groundwater flow in fracture rock assumes that, over some representative volume, the fractured media may be represented as an equivalent homogenous porous medium with groundwater flow governed by Darcy's law (Selroos *et al.*, 2002). Past thesis research (Staples, 2002) has shown that the equivalent porous medium (EPM) model may be appropriate for application in some fractured systems.

Recently, models have been developed that explicitly account for the geometry of each fracture, making it possible to simulate field-scale flow and transport involving thousands of fractures (Wellman and Poeter, 2003). These so-called discrete fracture network (DFN) models are based on the premise that groundwater flow and transport in rocks occur primarily within fractures. This approach simulates individual fractures in the rock and then solves the equations that describe groundwater flow and contaminant transport in the interconnected system of fractures (Selroos *et al.*, 2002).

1.3 Research Objective

Understanding flow and transport in fractured rock is essential for assessing the groundwater resources of fractured aquifers and predicting the movement of hazardous chemicals if and when contamination occurs (Department of the Interior, 2004). The goal of this research is to ascertain if currently available models can be used as tools in managing groundwater contamination in fractured aquifers. The research will focus on answering the following questions:

1. What models are currently available to simulate dissolved contaminant transport in fractured media?
2. What criteria may be used to decide whether a model is applicable for use at a particular contaminated fractured site? Are the necessary data (hydrogeologic, monitoring, *etc*.) available at a typical DoD hazardous waste site?
3. Given the state-of-the-art of fractured system modeling, how confident are we in the ability of these models to "adequately" simulate transport in fractured systems?
4. How might a fractured system model be used to manage contaminated fractured media sites?

1.4 Research Methodology

In order to effectively answer the above questions, the step-by-step method outlined below will be followed.

1. Conduct a literature review to investigate characteristics of fractured aquifers and the state-of-the-art of fractured transport modeling.
2. After selecting an appropriate fractured model that can be applied to a reasonably well-characterized site, build confidence in the model by using it to simulate hydrologic and contaminant data from the site. Such data may be available from Ramstein AB, Spangdahalem AB, Osan AB, Loring AFB, and Pease AFB.

3. Using data from the fractured site (either the same site that was used in step 3 or a different site), demonstrate how the model could be applied to manage contamination at the site.

1.5 Scope and Limitations

This research is limited to the evaluation of models specifically applicable to modeling flow and transport within fractured aquifers. The results of this study will provide scientists, engineers, and decision makers with information on model performance and ease of use. Specific limitations are as follows:

1. Contaminant and hydrogeologic data from DoD installations residing over fractured media are somewhat limited. Therefore, data that are available will be used to make generalizations regarding contaminant hydrogeology.
2. This study will be restricted to available data. There will be no new field investigations.
3. There will be a single interpretation of the site with a well defined domain. There will be a controlled data set with specific values of key parameters.
4. This study will only use the selected model and personal experience of contributing parties and will not involve any optimization.

2 Literature Review

2.1 Introduction

Groundwater is one of the United States' most important natural resources. Roughly one-half of the population relies on groundwater for drinking and other domestic purposes, and over 40% of irrigation water is supplied from groundwater (Konikow, 1995). Data collected on water use in the United States show increasing groundwater withdrawals, and from 1950 to 1990, withdrawals have doubled from 34 to 79.4 billion gallons per day (Solley *et al.*, 1993).

With the nation's increased demand for water, communities are turning to fractured aquifers for supply. Much of the Northeast, Southeast, and mountain West rely heavily on fractured aquifers for groundwater supply (USGS, 2004). Understanding groundwater flow and contaminant transport in these aquifers is an area of research that is rapidly gaining importance. Historically, groundwater research has focused on flow and transport in porous media rather than in fractured rock systems. The theory of flow through porous media began with the publication of Henri Darcy's experimental work in 1857 (USEPA, 2002). By comparison, the first comprehensive study of fractured flow was sponsored in 1950 by the oil industry to aid their attempts to increase oil production by fracturing the reservoir (Gale, 1982).

The importance of understanding flow and transport in fractured systems is of growing concern to the Department of Defense (DoD) and the United States Air Force (USAF). Information provided by the Citizen's Clearinghouse for Hazardous Waste states the DoD may be the largest hazardous waste generator in the country (Bedient et

al., 1999). The DoD produces over one billion pounds of hazardous waste per year, which is more than the combined production of the top five civilian chemical companies. The USAF alone estimates there are more than 4,300 waste sites at over 100 of their bases (Bedient *et al*., 1999). The contamination at a number of these sites is so severe that the bases have been placed on the National Priority List as Superfund sites. The Strategic Environmental Research and Development Program (SERDP) and the DoD Environmental Security Technology Certification Program (ESTCP) estimate that 1/3 of the DoD chlorinated solvent contaminated sites, including two large Superfund sites at Pease and Loring Air Force Bases, reside over fractured aquifers. Because of the scope of the problem of contaminated fractured aquifers within the DoD, SERDP and ESTCP have encouraged research that will result in models and increased understanding of fractured flow and transport (SERDP/ESTCP, 2002).

2.2 Background

To support sound decisions by managers tasked with dealing with contaminated fractured aquifer systems, an understanding of fluid flow and contaminant transport in those systems is critical. Fractured geological formations are common throughout the world and are of interest in a number of contexts: water supply exploitation, subsurface contamination, and petroleum reservoir development to name a few. In this study, we will focus on hydrogeological issues related to water quantity and quality. Fractures are the principal pathways for flow and transport of water and contaminants through otherwise impermeable or low permeability rocks. We will review the physical factors that control flow and transport behaviors, examine common models used to describe the

behaviors, and discuss the integration of conceptual pictures, models, and data (Berkowitz, 2002). In the following section, we review the properties of fractured rock and the physical factors that control flow and transport through this type of media.

2.2.1 Properties of Fractured Rock

Fractured rock, such as limestone, siltstone, shale, and basalt, may be described as intact rock bodies separated by discontinuities (or fractures) (Domenico and Schwartz, 1998). For the purposes of this study, fractures refer to all cracks, fissures, joints, and faults that may be present in a formation and have the ability to transmit water and contaminants through discrete channels that may be interconnected to form an integrated system. Major factors affecting groundwater flow through fractured rock include fracture density, orientation, effective aperture width, and the nature of the rock matrix. Fracture density (number of fractures per unit volume of rock) and orientation are important determinants of the degree of interconnectedness of fracture sets, which is a critical feature contributing to the hydraulic conductivity of a fractured rock system (Witherspoon *et al*., 1987).

Only interconnected fractures provide pathways for groundwater flow and contaminant transport. Figure 2.1 illustrates the importance of fracture connectivity in rock. In figure 2.1a, there are numerous clusters of fractures, yet none of the clusters are connected, thus this system, although highly fractured, prevents groundwater flow through the system. Figure 2.1b shows clusters of fractures that are connected, which suggests groundwater flow is possible through this system (Domenico and Schwartz, 1998). Fractures oriented parallel to the hydraulic gradient are more likely to provide

effective pathways than fractures oriented perpendicular to the hydraulic gradient (EPA, 2002).

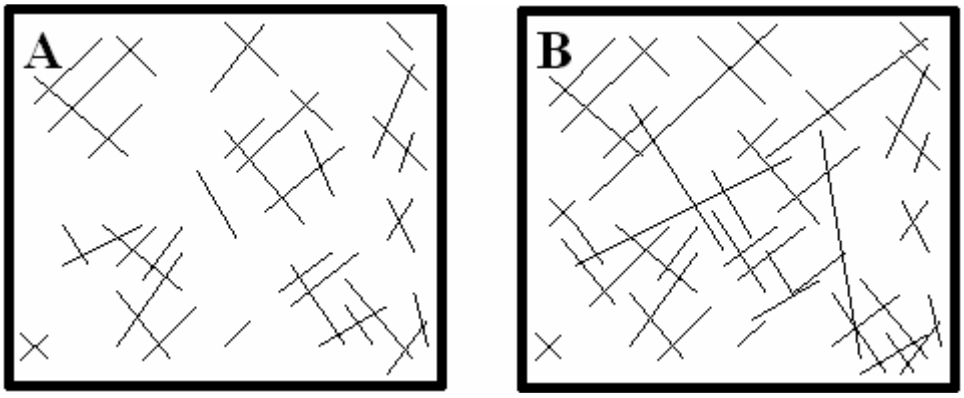

Figure 2.1: Connectivity in fractured media. (a) Unconnected fractures with minimal flow and (b) connected clusters that would support fractured flow (From Domenico and Schwartz, 1998)

The rock matrix (see Figure 2.2) plays an important role in the movement of water and contaminants through fractured rock systems. In essence, the rock matrix is a system of numerous fractures surrounded by an unfractured rock mass. The unfractured rock mass accounts for much of the porosity (storage) of the medium but little of the permeability (defined as the ability of a material to transmit fluids through its pores when subjected to pressure or a difference in head). Conversely, fractures may have negligible storage, but high permeability (Diodato, 1994).

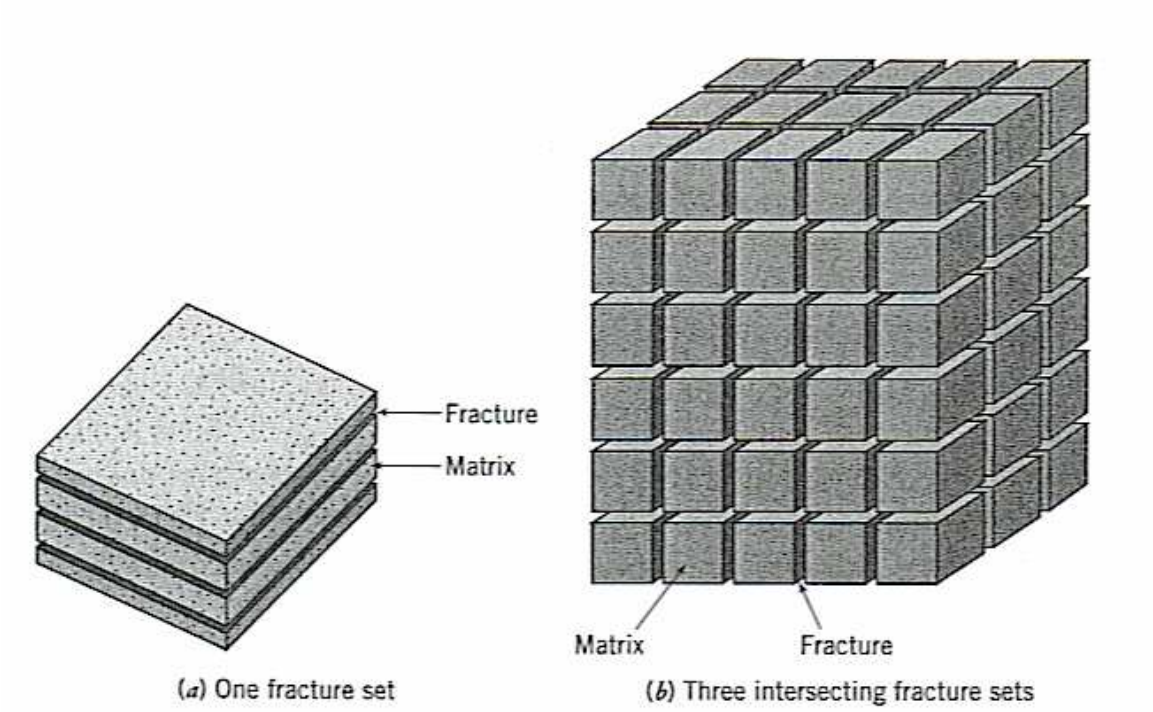

Figure 2.2: Schematic diagram of rock matrix system (From Schwartz and Zhang, 2003)

High porosity within the matrix would allow for significant storage of water and contaminants. Fractures account for the majority of permeability within the system and allow significant flow of water through the system. Rates of contaminant migration into and out of the rock matrix will depend on the porosity of the matrix and the matrix diffusion coefficient of the contaminant (EPA, 2002).

A complete description of a contaminated fractured rock system would include a tremendous amount of data. Information would include the length, aperture width, location, and orientation of fractures; the hydraulic head throughout the system; the porosity and permeability of the rock matrix; the sources of water and contaminants; the nature and concentrations of the contaminants throughout the system; and the chemical interactions between the contaminants and the rock matrix (EPA, 2002). Currently, the

collection of such detailed information is technically impossible on the scale of most contaminated sites. In general, the more detailed the site characterization, the greater the probability of success in modeling the site. The accuracy of flow and transport modeling in fractured rock systems is highly dependent on the accuracy and extent of site characterization data (EPA, 2002).

2.2.2 Flow in Fractured Rock

The first comprehensive study dealing with flow through open fractures was done by Lomize (1951). The study tried to experimentally determine the relationship between flow through a simple fracture and fracture properties. Based on the study, it was determined that the local flow rate through a single fracture is dependent on the hydraulic conductivity of the fracture, whether flow is laminar or turbulent (*i.e.*, the value of the Reynolds' number), the fracture aperture width, and the roughness of the fracture walls (Thiel, 1989).

Flow through a fracture is generally idealized as laminar flow between a pair of smooth, parallel plates. This idealization results in the "cubic law," (see equation 1)

$$T_{fr} = -\left(\frac{\rho g}{\mu}\right)\cdot\left(\frac{b^3}{12}\right) = K_{fr}\cdot b \qquad \text{.....(1)}$$

which states that the transmissivity (T_{fr}) or hydraulic conductivity (K_{fr}) of a fracture can be determined from the fracture aperture width (b), the fluid density (ρ) and viscosity (μ), and the gravitational constant of acceleration (g). It is also noted that ($b^3/12$) represents the permeability of the fracture (Snow, 1965). This relationship was theoretically

deduced assuming that fluid percolates through a smooth aperture under saturated, laminar, incompressible flow conditions (Lee and Farmer, 1993).

As seen in Equation 1, the cubic law relates the local flow rate through the fracture to the cube of the fracture aperture width (Snow, 1965). The equation assumes matrix permeability is negligible, and as a result, assumes all flow occurs through the fracture (Witherspoon *et al.*, 1980). A full derivation of the cubic law can be found in Bear et al. (1993).

The validity of the cubic law has been the subject of much debate over the years. A number of laboratory experiments (Durham and Bonner, 1994; Keller *et al.*, 1995; Vandergraaf, 1995) and field studies (Rasmuson and Neretnieks, 1986; Novakowski *et al.*, 1985) on flow through fractures indicate the cubic law may not be adequate to describe flow. Gale and Raven (1980) showed the cubic law is not applicable when deformable natural discontinuities lead to varying contact area that result in significant changes in the flow rate. Gale *et al.* (1985) showed that when fracture surfaces are not in contact (i.e., natural deformations of the fracture walls do not touch) existing laboratory data supported the use of the cubic law with appropriate corrections for roughness. Tsang (1984) experimentally showed a one to two order-of- magnitude error in estimating flow if the tortuosity of the flow path is neglected.

The cubic law has been extended over the years, to account for surface roughness and seepage into the rock matrix (Basha and El-Asmar, 2003). However, though more advanced conceptual models have been introduced in recent years, an alternative to the cubic law has yet to be generally accepted (Berkowitz, 2002).

2.2.3 Solute Transport in Fractured Rock

Measurement and quantitative analysis of solute transport in fractured systems remains one of the most challenging problems in subsurface hydrology (Berkowitz, 2002). This section will discuss the various approaches that have been used to quantify transport of contaminants within fractured systems. Both conservative and reactive solute transport will be discussed.

2.2.3.1 Conservative Solute Transport

The principal modeling approach applied to quantify transport of conservative solutes is the classic advection-dispersion equation (ADE) (Berkowitz, 2002). Although use of the ADE is convenient, Becker and Shapiro (2000) have shown that breakthrough curves in fractures exhibit behavior different than the classic S-shaped breakthrough curves predicted by the ADE for transport in homogeneous media. The breakthrough curves in fractured media typically exhibit early initial arrival times, with one or more sudden jumps in concentration, and/or long tails.

In fractured rock, the overall permeability of the fractures is generally larger than that of the rock matrix. As a result, fluid and contaminant velocities are significantly higher within the fractures, and the solute may bypass the matrix and migrate further downstream. Advection is generally assumed to dominate the system (Berkowitz, 2002). The diffusive interaction between fracture and matrix exerts a strong control on solute movement and can account for retardation of the contaminant; however, the significance of this interaction in the field is not well known (NRC, 2001).

Another important feature of transport in fractured domains is complex dispersion. In general, dispersion is assumed negligible due to the dominance of

advective transport in fractures (Berkowitz, 2002; Kim *et al.*, 2004). de Josselin de Jong and Way (1972) and Way and Mckee (1981) provided a theoretical analysis of dispersion in fractured media. Their system consisted of two sets of fractures equally spaced, infinite in length, and having constant aperture width. Their results showed dispersion was complex with directions of spreading at angles to the direction of mean flow. Gelhar *et al.* (1992) and Schwartz and Smith (1988) performed similar studies with discontinuous fractures of finite length and variable aperture width and confirmed the complex behavior of dispersion whereby the evolution of a migrating plume cannot be quantified by a constant center of mass velocity and constant dispersion coefficients, as is typically done to characterize advective/dispersive transport in porous media.

Recently, Berkowitz and Scher (1997, 1998) introduced continuous time random walk (CTRW) theory to quantify transport in fractured and heterogeneous porous media. CTRW theory accounts for this complex (non-Fickian) dispersion behavior that cannot be properly quantified by the use of the ADE. CTRW simulates contaminant migration as particles traverse different paths with spatially changing velocities. This kind of behavior is represented by a joint probability density function, $\psi(s,t)$, which describes each particle "transition" over a distance, s, in time, t. The CTRW theory appears to be a promising means to quantify a wide range of dispersive transport behavior in fractures (Berkowitz, 2002).

Another transport issue is describing the behavior of solute at fracture junctions. In general, either complete mixing or streamline routing is assumed (Park *et al.*, 2003). The complete mixing idealization assumes the residence time of solute at an intersection is long enough to ensure equal solute concentrations in the outlet branches. The

streamline routing assumption allows the solute to move along streamlines without any mixing (Wilson and Witherspoon, 1976). Park *et al.* (2003) assessed the importance of fracture intersection mixing assumptions on simulated solute migration patterns. Comparison of the outcomes showed that solute transport is strongly influenced by the geometry of the network and the choice of mixing assumptions at fracture intersections is of little importance.

Field scale tracer tests have been carried out over the last two decades and demonstrated that even highly detailed geological and hydraulic characterization of fractured formations is generally insufficient to allow reliable, quantitative prediction of solute migration (Smellie and Laaksoharju, 1992; Hadermann and Heer, 1996). The degree of fracture connectivity is extremely difficult to characterize, and leads to unexpected appearance of tracers at some wells and anomalous arrival times at other wells. As such, the ability of available models to simulate solute transport remains the subject of continued debate (Berkowitz, 2002).

2.2.3.2 Reactive Solute Transport

The vast majority of studies on solute transport in fractured media have focused on the behavior of conservative chemicals. In addition to the physical transport mechanisms discussed in the previous section, there are a wide range of reactive transport mechanisms present within a fracture, along the fracture walls, and/or within the adjacent porous rock matrix. These processes include adsorption/desorption, dissolution/precipitation, radionuclide decay, organic reactions and volatilization, and/or biotransformation. Most studies to date have focused on the influence of

adsorption/desorption mechanisms on solute transport in fractured media (Berkowitz, 2002) and this mechanism will be reviewed here.

Freeze and Cherry (1979) developed a simple model accounting for adsorption along planar fracture walls. A retardation factor is defined based on the product of a distribution coefficient, Ka, and the surface to void space ratio, A. Ka is defined as the mass of solute on the solid phase per unit area of solid phase divided by the concentration of solute in solution. Therefore, the retardation equation for fractured systems becomes:

$R = 1 + AK_a$……..…(2)

If the fracture aperture width, b, can be determined, and the fracture surface is assumed to be planar, A= 2/b. Although Equation 2 is simple in conceptual terms, it is difficult to apply to field systems. Fracture surfaces usually are non-planar, and without elaborate experimental effort, the actual surface area with which the contaminant reacts is unknown (Freeze and Cherry, 1979).

More sophisticated models must be developed to account for sorptive transport in fractured media in a computationally tractable manner. In general, the state-of-the-art is to assume a single, overall retardation coefficient for the fractured system (Berkowitz, 2002).

2.3 Modeling Methods

As stated in section 2.1, SERDP and ESTCP have called for research to better understand and model fractured flow and transport (SERDP/ESTCP, 2002). In order to deal with the wide variety of flow and transport problems associated with fractured systems, a number of modeling approaches have been developed. These models can

account for a range of possible fracture distributions, hydraulic characteristics, rock matrix properties, and flow and transport processes. These modeling approaches are typically divided into two classes: continuum models and discrete fracture models (Berkowitz, 2002). Flow in fractured media is typically simulated using one or more of the following conceptual models: (1) equivalent porous medium (EPM), (2) dual continuum, (3) triple continuum, (4) discrete fracture network (DFN), or (5) hybrid DFN/EPM approaches. Following a short review on model development, each of these models is discussed in detail below.

2.3.1 Model Development

A groundwater model is designed to represent a simplified version of an actual field site. It attempts to translate our understanding of physical, chemical, and biological processes into mathematical terms (Bedient *et al.*, 1999). The first step in the modeling process is the development of a conceptual model which consists of a description of the physical, chemical, and biological processes thought to govern behavior in the system being analyzed. The next step is to translate the conceptual model into mathematical terms. The mathematical model is a set of equations associated with certain boundary conditions that describe the conceptual model (Bedient *et al.*, 1999).

Anderson and Woessner (1992) propose the modeling protocol summarized below:

1. Establish the purpose of the model.
2. Develop a conceptual model of the system.
3. Select the governing equations and computer code.

4. Design the model. This step involves creating the grid, selecting time parameters, selecting initial and boundary conditions, and estimating model parameters.

5. Calibrate the designed model. Establish that the model can reproduce field measured values.

6. Determine the effects of uncertainty on model results. Model parameters are varied to evaluate the effect on model performance.

7. Verify the calibrated model. Test model ability to reproduce field measurements.

8. Predict results based on calibrated model.

9. Present modeling design and results

10. Post audit and redesign as necessary. Compare model predictions against new field data which might lead to further modifications and refinements of the model.

Following the above protocol increases the confidence in modeling results and allows scientists, engineers, and remediation project managers access to an effective decision making tool (Bedient *et al.*, 1999).

2.3.2 Equivalent Porous Medium (EPM)

The EPM approach treats the fractured rock system as if it were an unconsolidated porous medium. This approach is most likely to be successful when the spacing of the fractures is small compared to the scale of the system being studied and when the fractures are interconnected (EPA, 2002). As the name suggests, fluid flow through a fractured material can be simulated by representing the fractured medium as a porous medium with equivalent hydraulic properties (Figure 2.3). Hydraulic parameters (*e.g.*, porosity, hydraulic conductivity) are selected so the flow behavior simulated in the EPM represents the actual flow observed in the fractured system.

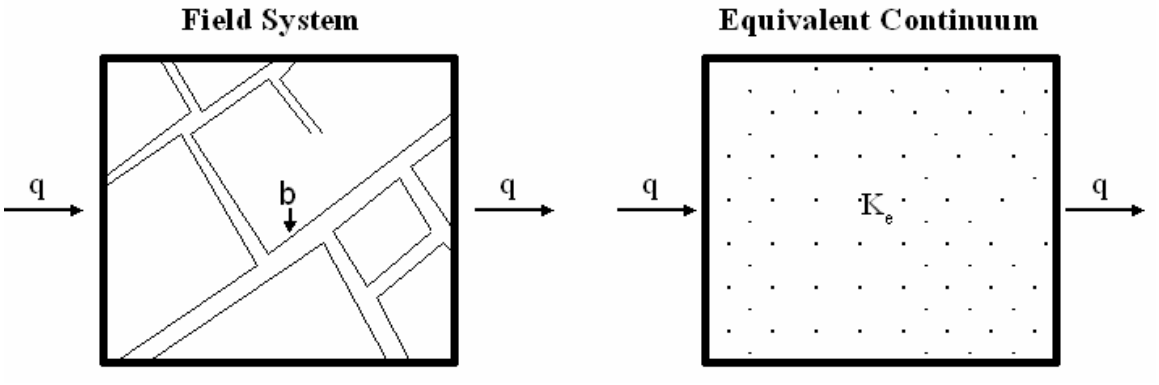

Figure 2.3: Conceptual models of a fractured rock system. Simplified network with aperture "b" and flow "q" from left to right and equivalent porous media model of field system (From Anderson and Woessner, 1992)

An EPM approach assumes the fractured material can be treated as a continuum and a representative elementary volume (REV) of material characterized by effective hydraulic parameters can be defined. The concept of selecting an REV is illustrated in Figure 2.4. The plot shows hydraulic conductivity (K) versus the sample volume. At the microscopic level, as the volume increases, there is considerable fluctuation of the values for K. However, when the sample becomes very large, there are no longer any significant variations in the value of K with respect to the volume. This model requires that effective values of hydraulic conductivity, specific storage, and porosity in the fractured material be defined, for use in the EPM. Values for these parameters can be derived from aquifer testing, estimated from water balances or inverse models, and/or calculated from field descriptions of fracture apertures, lengths and interconnections, and unfractured rock volumes and permeabilities (Anderson and Woessner, 1992).

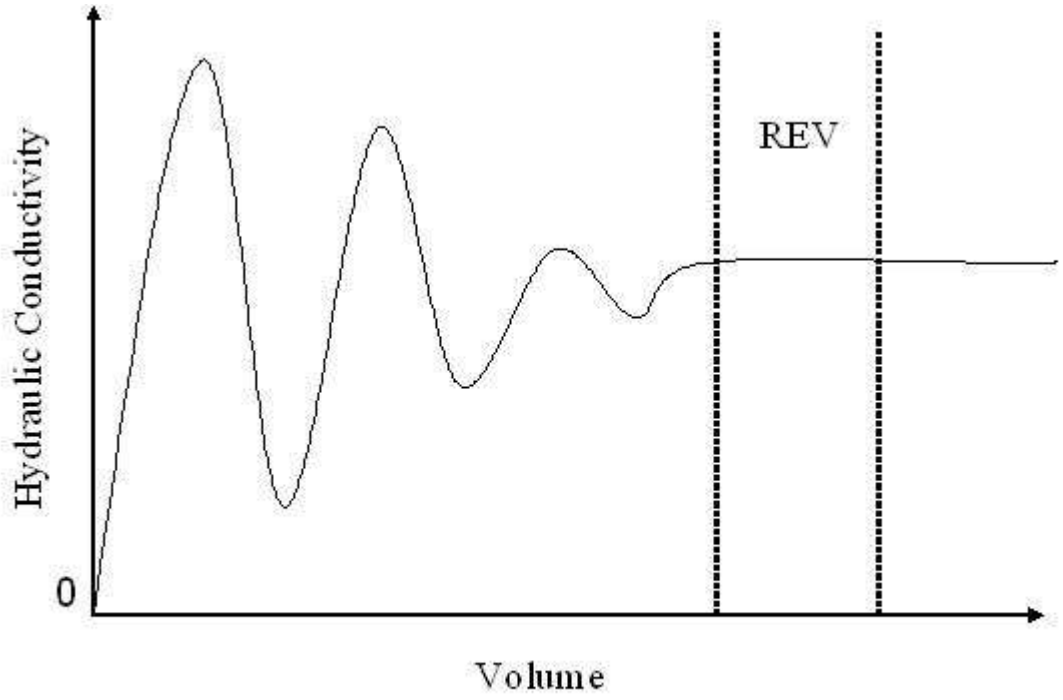

Figure 2.4: Variation in hydraulic conductivity (K) as a function of volume. The dashed lines indicate where the assumption of an REV is valid. (From Domenico and Schwartz, 1998)

The difficulty in applying the EPM approach arises in determining the appropriate size of the REV needed to define the equivalent hydraulic properties. When fractures are few and far between and the hydraulic conductivity is low, the EPM method may not be appropriate, even with a large REV. The EPM approach may adequately represent the behavior of a regional flow system, but poorly represent local conditions (Anderson and Woessner, 1992).

Pankow *et al.* (1986) compared two contaminated fractured rock sites. The two sites differed in regard to fracture aperture, fracture spacing, matrix porosity, and matrix diffusion coefficient. They concluded that the EPM approach worked well in describing contaminant transport in the system with small fracture spacing (high fracture density). In addition, the system had a high enough matrix porosity and diffusion coefficient to

rapidly establish matrix/fracture equilibrium. They also concluded that the EPM approach would not be appropriate for the other system where there was low fracture connectivity and density. In this system, matrix/fracture equilibrium was not rapidly established and the EPM was deemed inappropriate.

In a similar study, Lee and Lee (1998) applied an EPM to characterize flow in a fractured system in South Korea. They found that in order to use an EPM to analyze a fractured aquifer, three conditions must be met: (1) small fracture spacing (high fracture density), (2) high fracture connectivity, and (3) random fracture orientation. These criteria were tested by analyzing rock cores taken from various wells. The cores contained no dominant fractures and showed high fracture densities. In addition, pump test data closely matched Theis drawdown curves. Lee and Lee (1998) concluded that the EPM was valid for the system.

It has been shown that under certain scenarios, the EPM model was inadequate, but overall, EPM has been used with success in the past and generally models the response of fractured systems adequately for design purposes (NRC, 1990; EPA, 2001).

2.3.3 Dual-Continuum Model

The dual-continuum method (see figure 2.5) has been used to characterize flow in fractured media. Two subsets of this method are the dual porosity method, which assumes no flow between matrix blocks, and the dual permeability method, which allows for flow between matrix blocks (Huang *et al.*, 2004).

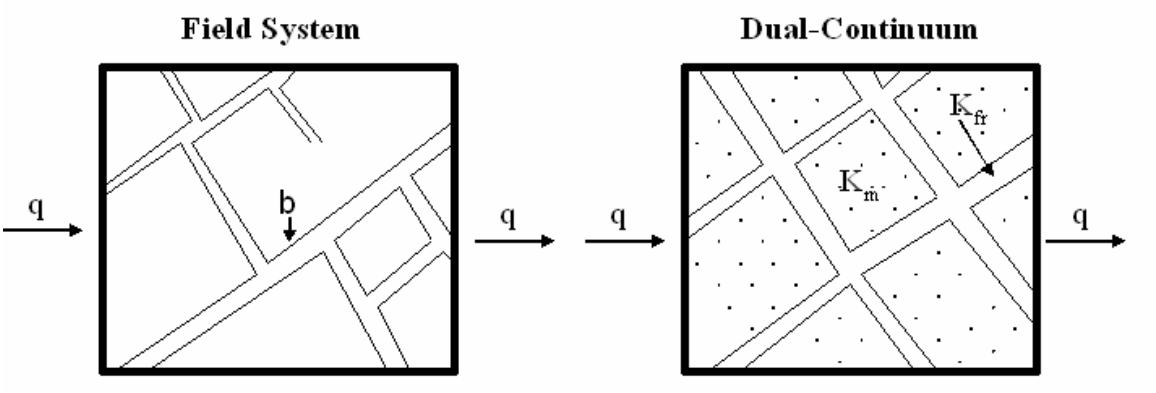

Figure 2.5: Conceptual models of a fractured rock system. Simplified network with aperture "b" and flow "q" from left to right and dual-continuum model of field system (From Anderson and Woessner, 1992)

In the dual porosity model, a flow domain is composed of matrix blocks with negligible permeability, embedded in a network of interconnected fractures, with global flow and transport in the formation due only to the fracture system, which is conceptualized as an effective continuum (Barenblatt et al., 1960; Warren and Root, 1963). The model treats matrix blocks as spatially distributed sinks or sources which allow for diffusion of contaminant into and out of the fracture system and the fracture–matrix interflow is treated as a quasi-steady state (Wu *et al.*, 2004).

In an attempt to incorporate additional matrix–matrix interactions, the dual-permeability model has been developed. This type of dual-continuum model considers global flow occurring not only between fractures but also between matrix blocks. In this approach, the fractures and the matrix are each represented by separate blocks that are connected to each other. The same quasi-steady state flow assumption as that in the double-porosity concept is used to handle fracture–matrix interflow (Wu *et al.*, 2004).

In general, the dual-continuum system is modeled as if it were composed of two overlapping continua with different porosities and permeabilities. Low porosity and high

permeability are associated with the fractures while high porosity and low permeability are associated with the rock matrix. The model allows for transfer of contaminants between the fractures and the rock matrix. The fractures are considered the more permeable system and transmit groundwater to the well, while the less permeable rock matrix has a high storage coefficient and acts as a source or sink (Hamm and Bidaux, 1996; Lee *et al.*, 2001).

No account is taken of the arrangement of fractures and their relation to one another; instead, it is assumed there is a mixing of fluids in the interacting continua (NRC, 1990). When developing this model, the proportions of fracture flow and matrix flow can be determined by the solution of two sets of flow equations using coupling parameters to represent flow between the matrix and fractures. The systems are interconnected, so the loss of fluid in one porous system represents a gain in the other (Lee and Farmer, 1993).

Applicability of the dual continuum approach is generally dependent upon: (1) the fractures being closely spaced relative to the size of the system, (2) relatively uniform distribution of fracture networks (high degree of fracture connectivity), and (3) knowledge of fracture and matrix properties (Preuss and Narasimhan, 1985; Wu *et al.*, 2004).

2.3.4 Triple Continuum Model

The triple continuum model (see Figure 2.6) was developed to investigate the impact of small-scale fractures on flow and transport processes in fractured rocks. This new conceptual model subdivides fractures into two types: large-scale and small-scale.

Large-scale fractures are those responsible for global connections, while small-scale fractures are those that provide large fracture storage space and enhance the local connections to the matrix system without contributing to global flow or transport (Wu *et al.*, 2002).

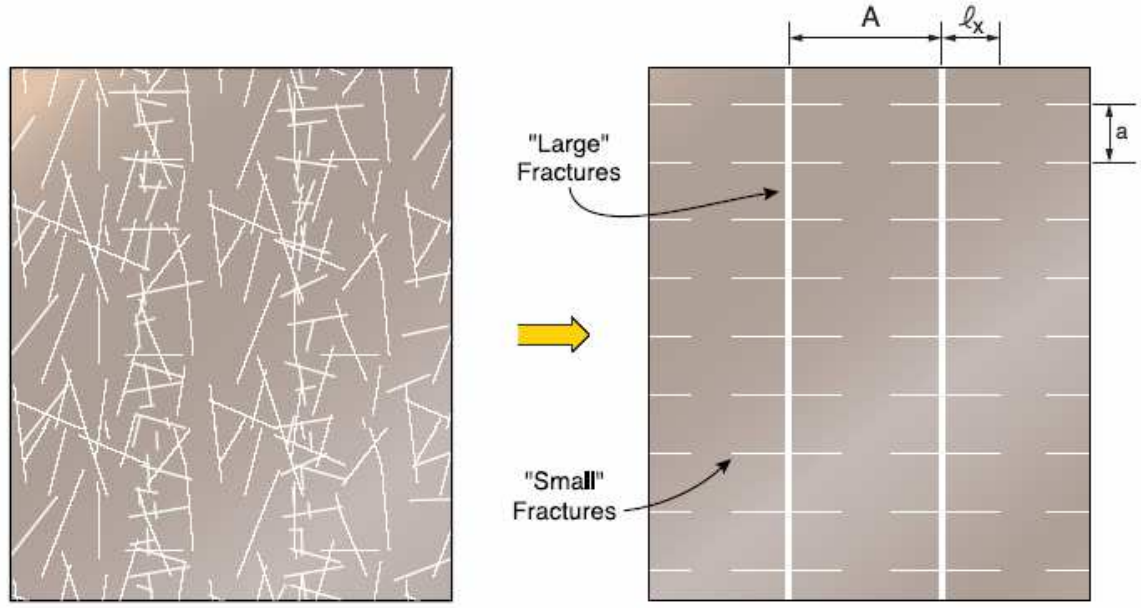

Figure 2.6: Basic conceptualization for triple continuum approximation of a field system (from Wu et al., 2004)

Typically, the triple-continuum model, like the dual-continuum approach, uses an effective porous medium to approximate the two types of fractures and the rock matrix, and considers the three continua to be spatially overlapped. Like other continuum approaches, the triple-continuum model relies on the assumption that approximate equilibrium exists (locally) within each of the three continua at all times at a given location (Wu *et al.*, 2004). The model formulation uses three sets of conservation equations to describe flow and transport processes at each location of the system (Wu *et al.*, 2002).

Wu *et al.* (2002, 2004) implemented the triple continuum model to examine field problems at Yucca Mountain, Nevada. It was shown that in a fracture–matrix continuum containing both large-scale globally connected fractures and small-scale locally connected fractures, the main role played by the small fractures is to control fracture–matrix interflow and transport processes by enlarging effective fracture–matrix interface areas and offering intermediate storage space. The study indicated that the transient effects of small fractures on flow and transport is significant and cannot be generally ignored.

Wu *et al*. (2002, 2004) determined that if small-fracture permeability is similar to matrix permeability or very few small fractures exist (i.e., the small-fracture porosity is near zero), the triple-continuum model collapses to a dual-permeability model, and the traditional dual-continuum model should be used instead. On the other hand, if small fractures are extensive and well connected to larger fractures, fracture–matrix equilibrium will be reached relatively quickly, and the fractured system may behave as an equivalent porous medium.

Introducing the third continuum to the dual-continuum model to build a triple-continuum model requires one more fracture–matrix property set for small fractures. This additional property set makes the triple-continuum model more difficult to use than a dual-continuum model (Wu *et al.*, 2004).

2.3.5 Discrete Fracture Network (DFN)

According to the REV concept (see section 2.3.1), there exists a scale at which individual heterogeneities and discrete features can be ignored, due to a process of

averaging to produce an equivalent porous medium. The fundamental motivation of discrete fracture network (DFN) modeling is the recognition that at every scale, groundwater transport in fractured rocks tends to be dominated by a limited number of discrete pathways formed by fractures (Dershowitz *et al.*, 2004). Discrete fracture models allow quantification of many flow and transport phenomena that are not adequately captured by use of continuum models. A major advantage of the discrete fracture approach is that it can explicitly account for the effects of individual fractures on fluid flow and transport (Berkowitz, 2002).

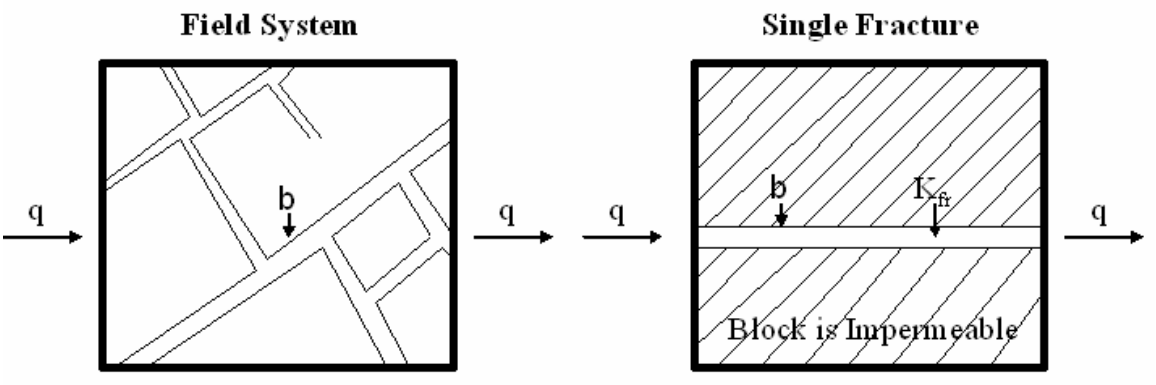

Figure 2.7: Conceptual models of a fractured rock system. Simplified network with aperture "b" and flow "q" from left to right and discrete fracture network model of field system (From Anderson and Woessner, 1992)

Another major advantage of the discrete fracture approach (see Figure 2.7) is that the geometry of each fracture is explicitly included to account for the effects of individual fractures (Berkowitz, 2002). Fractures are most often represented as channels with parallel sides, and the individual fractures are combined into fracture networks. The simplest network has a set of parallel fractures in a one-dimensional problem. A more complex network has two sets of parallel fractures oriented at some angle to each other in a two-dimensional array (Smith and Schwartz, 1984). Another increase in complexity,

and one step closer to reality, is to allow the fractures to have varying lengths, locations, and orientations relative to one another (Long and Billaux, 1987). These models can have either two- or three-dimensional fracture arrays. Some of the discrete fracture models only account for solute transport by advection, and others include both advection and dispersion. Essentially all of the discrete fracture models are research models (EPA, 2002).

One obvious problem in the practical application of discrete fracture models is that it is almost impossible to define the fracture system at a site in fine enough detail to apply the model (EPA, 2002). Additionally, there are computational limitations based on the size of the site under study (Berkowitz, 2002). DFN flow and transport modeling is limited to 10^4 to 10^5 fractures by computational constraints (Dershowitz *et al.*, 2004). Another limitation of the DFN approach is the lack of study into how an increase in stress with depth will cause decreases in pore pressure (dewatering) which results in a decrease in fracture aperture. To date, the DFN model has mainly been applied as a research tool (Anderson and Woessner, 1992).

The best potential for application of this approach seems to be to use statistical modeling of the fracture system to duplicate the measured hydrology at a site. Most of the work on complex discrete fracture networks has been done in connection with the disposal of nuclear waste in crystalline rocks and has not included diffusion into the rock matrix (EPA, 2002).

Cacas *et al*. (1990 a; 1990b) reported an application of a DFN flow and transport model to a granite uranium mine in France. The study inferred fracture density,

orientation, and fracture size from rock cores and rock outcroppings. Fracture hydraulic properties were inferred from local injection tests, and transport properties were inferred from tracer tests. The model assumed all fractures could be idealized as smooth parallel plates and utilized the cubic law discussed in Section 2.2.2 (Snow, 1965). Cacas *et al*. (1990 a; 1990b) note that a large number of data were used to construct the DFN.

2.3.6 Hybrid DFN/EPM Model

As discussed previously, there are two classes of fracture models: discrete fracture models and continuum models. It is interesting to note that in most cases, DFN models employ continuum approaches to treat flow and transport within each fracture. Also, continuum models can be applied to the investigation of discrete fractures within a system by representing them as heterogeneous layers in a continuous medium (Berkowitz, 2002). In this vein, there recently have been increasing developments of hybrid DFN/EPM models such as ConnectFlow (Serco, 2004) and FracWorks XP (Dershowitz *et al.*, 2004).

As the name suggests, the DFN/EPM model combines aspects of both DFN and EPM models. Figure 2.8 illustrates both portions of this model, with the colored polygons representing the DFN model and the grid representing the EPM model. The DFN model idealizes fractures as planar polygons because they are computationally efficient and typically few field data are available to describe non-planar fractures (Dershowitz *et al.*, 2004). The assumption of polygonal fractures allows the representation of a wide variety of fracture shapes by a single mathematical form. Previous studies of fracture mechanics in homogeneous rock suggest the general shape of

a single fracture should be elliptical (Baecher *et al.,* 1977). The Baecher model (Baecher *et al.,* 1977) locates fracture centers in space through a Poisson process and the fractures are generated as disks based on aperture and orientation. Rarely is a fracture perfectly elliptical in the field, and Dershowitz (1984) noted observed fractures are generally polygonal due to terminations at intersections with other fractures, and little error is introduced by representing the elliptical fracture as a polygon of equivalent area. The varying degrees of shading in Figure 2.8 represent varying values of hydraulic conductivity in the system with darker shading symbolizing less conductive fractures. The varying sizes of polygons represent different size fractures.

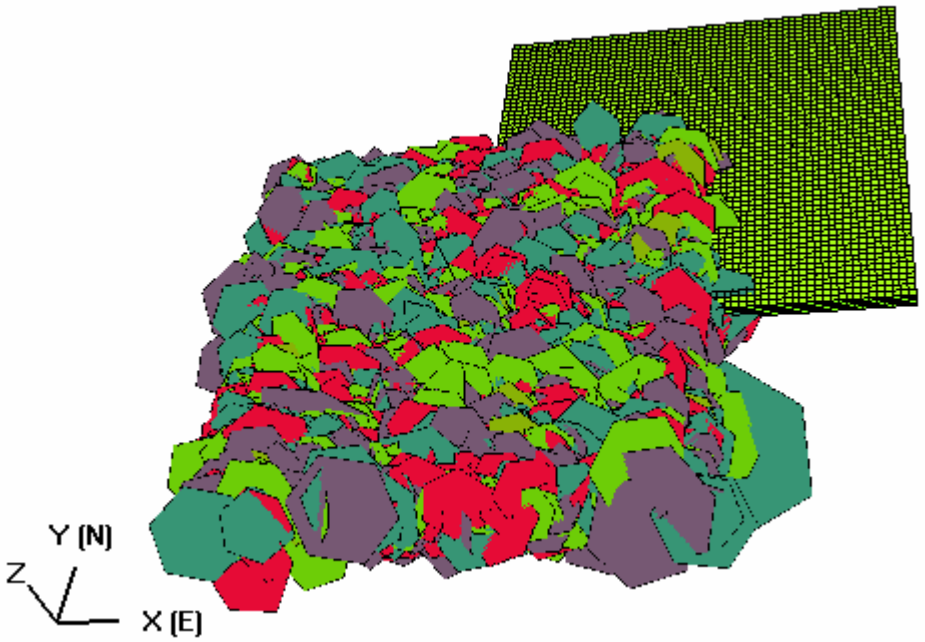

Figure 2.8: EPM implementation of a DFN hydrostructural model (From Dershowitz et al., 2004). The DFN model is represented by the colored polygons.

Figure 2.8 illustrates the EPM implementation of a DFN model, where an EPM grid (shown in the upper right hand portion of the figure) is conceptually merged with the

DFN model, so that each grid cell has properties related to the fracture network. The method used to calculate EPM properties from DFN fractures is commonly referred to as the Oda (1985) approach. The advantage of the Oda approach is that it can obtain EPM properties for grid cells based directly on the geometry and properties of the fractures within those cells. The Oda approach begins by generating the full, three dimensional DFN. While DFN flow and transport modeling is limited to 10^4 to 10^5 fractures by computational constraints, the Oda approach can be applied to patterns of 10^7 or more fractures. The Oda approach overlays an EPM grid on the fractures, and derives EPM properties for each grid cell based on the DFN contained in that cell (Dershowitz *et al.*, 2004).

For a specific grid cell with known fracture areas and transmissivities obtained from the DFN model, an empirical fracture tensor can be calculated by adding individual fractures weighted by their area and transmissivity (Dershowitz *et al.*, 2004). Oda's permeability tensor is then derived by assuming that fracture flow is a vector along the fracture's unit normal (Dershowitz *et al.*, 2004). The Oda approximation derives an equivalent permeability tensor, according to a specific grid. The permeability tensor can then be inserted into the cubic law to calculate hydraulic conductivity values for each cell. The Oda approach reproduces the underlying discrete fracture hydrostructural model for both flow and transport. This approach thus represents a balance between the accuracy of directly modeling each of the fractures in the hydrostructuctural model against the computational efficiency of coarser numerical model discretizations (Dershowitz et al., 2004).

The advantage of this approach is that it is able to more accurately model the response of the groundwater table and shallow wells using continuum EPM elements, while still using the DFN for evaluating connectivity between wells in the fractured rock (Dershowitz *et al.*, 2004). This model has been been applied in carbonate, fractured till, crystalline, and clastic systems. It is noted that the use of this model requires a dense fracture system with high connectivity (Dershowitz *et al.*, 2004).

2.4 Model Validation

Karl Popper (2002) once said that "scientific theory cannot be validated; only invalidated." This speaks to achieving absolute truth, which is virtually impossible when dealing with subsurface phenomena. Over the past several years, studies have shown that groundwater models are limited in their ability to predict system behavior due to substantial uncertainty inherent in the subsurface environment. Full characterization of the subsurface is needed to build a truly valid groundwater model, but obviously, full characterization of the subsurface is impossible—for instance, the massive extent of borehole drilling required for full characterization, even if economically feasible, would affect the integrity of the site just due to the number of holes that would be drilled (Hassan, 2004).

That being said, it becomes necessary to build confidence in groundwater models such that everyone involved, from the regulators to the public, agree the model is providing meaningful output to inform policy and remediation decisions. Popper (2002) argues that scientific theories can never be proven, merely tested and corroborated. In

this section, we will discuss the various philosophies and procedures on model validation and building confidence in groundwater models.

Currently, there are four proposed approaches to declaring a model as "valid." The first approach defines a valid model as one that truly represents reality. The second approach, which is related to the first, is based on the philosophical discussions of Karl Popper and states that models, as true representations of reality, can never be validated, but only invalidated. The third approach is a practical approach, defining a model as valid if there is confidence that modeling errors will have minimal effect on decisions or yield conservative results. Finally, the fourth approach acknowledges that although full scientific validation may be impossible, models can be accepted based on confidence that they yield reasonable results (Hassan, 2004).

Regardless of the validation approach, the cost of model validation should be considered when designing validation plans. Figure 2.9 shows a limit where additional validation costs contribute minimal increases in confidence. As such, decision makers must come to an agreement with regulators and the public as to level of confidence necessary (Hassan, 2004).

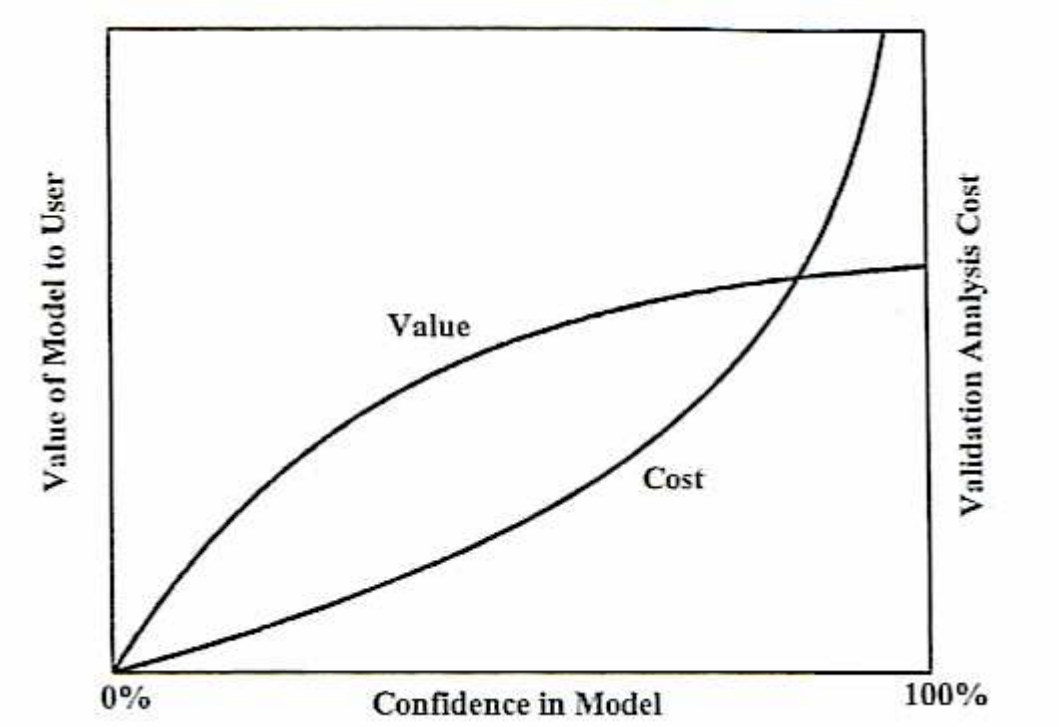

Figure 2.9: Value and cost of model as functions of desired level of confidence (From Hassan, 2004)

Once a level of confidence is agreed upon, the validation process can begin. Ultimately, validation requires a forward looking perspective. It is necessary to conduct the modeling process within an iterative loop of characterization, calibration, modeling, prediction, and recharacterization (Hassan, 2004). Figure 2.10 schematically represents this iterative loop (steps 1-6) and proposes an exit strategy. The inner loop represents the need to reduce the uncertainty of the model to negligible levels. There will never be enough information about a specific site to eliminate all model uncertainty. Therefore, a decision should not be based solely on this loop (Hassan, 2004). Rather than spend time recharacterizing the model through steps 1-6, it is better to accept some uncertainty and exit this iterative loop. The validation process now evaluates how the model conforms to

regulatory requirements and allows for reintroduction to the iterative loop as needed (Hassan, 2004).

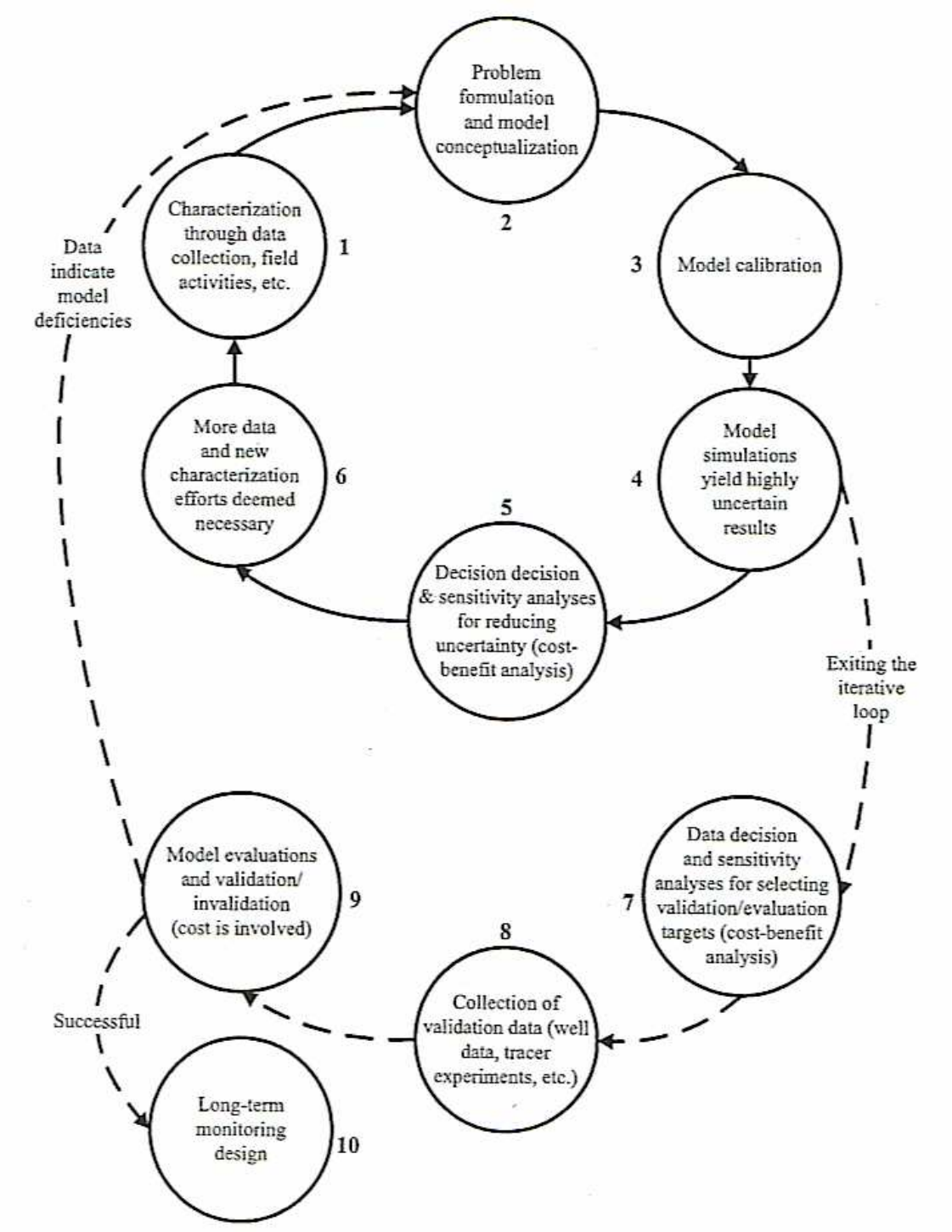

Figure 2.10: Flowchart of model validation plan (From Hassan, 2004)

In general, validating a site-specific model is difficult, but it is possible to build confidence in the model by following the simple flowchart presented above. Through the incremental collection of site specific information and reevaluation, the confidence in model results will increase and allow all concerned parties to make informed decisions about remediation alternatives. In Chapter 3, a model of an existing contaminated site will be built based on actual site hydrogeologic data. The model will be validated by comparing contamination data measured in the field with model-simulated contaminant concentration values.

3 Methodology

3.1 Introduction

Chapter 2 discussed various modeling methods which can be applied to simulate fractured aquifer systems. As shown in Chapter 2, the equivalent porous media (EPM) model has been extensively used to represent fractured flow systems. As was also noted in Chapter 2, perhaps the main challenge in applying an EPM model to simulate a fractured system is deciding upon appropriate parameter values to use in the model. In this chapter, we propose use of a hybrid discrete fracture network/equivalent porous medium (DFN/EPM) model to simulate contaminant transport in a fractured aquifer system. The DFN module is used to determine appropriate parameter values for input into an EPM model of the aquifer. As will be discussed in detail below, the DFN/EPM approach was chosen because it permits simulation of a fracture system without the extensive data collection (and costs) needed to characterize a site in order to apply a dual-porosity or DFN model.

Following the research methodology outlined in Chapter 1, after selecting an appropriate modeling approach, the next steps are to calibrate the model using contaminant data from a fractured aquifer site and then demonstrate how the model may be used to manage contamination at the site. This chapter will discuss the formulation of such a model. We first describe the process used to select a fractured aquifer site for study. After selecting a site, we provide the rationale for using the DFN/EPM approach for modeling the site. We then apply the FracWorks XP implementation of the DFN/EPM approach to construct a site model. Finally, we present our proposed

approach for calibrating the model and then use it to simulate the effectiveness of pump-and-treat remediation of the site.

3.2 Site Selection

3.2.1 Candidate sites

A number of Air Force installations were considered for this study. The installations were Ramstein Air Base (AB), Germany; Spangdahalem AB, Germany; Osan AB, Republic of Korea; Pease Air Force Base (AFB), New Hampshire, and Loring AFB, Maine. Because of the data necessary to model fractured aquifer sites, several of the installations were eliminated from this study. Ramstein AB and Spangdahalem AB both supplied detailed hydrogeologic data, but no historical contaminant monitoring data were available. Osan AB supplied both hydrogeologic and historical contaminant monitoring data, and this site has recently been studied using the EPM approach (Staples, 2002). However, the data were not well organized, consisting largely of hard copies of reports, well logs, concentration measurements, and pump tests. Pease AFB supplied both hydrogeologic data and detailed contaminant monitoring data in digital form; therefore, this study will focus on applying the relatively new hybrid DFN/EPM model to the fractured aquifer located below Pease AFB in Portsmouth, New Hampshire.

3.2.2 Site Description

This study will examine one of the Installation Restoration Program sites located on Pease AFB (see Figure 3.1). Site 32 encompasses Building 113 in the center of the

base in the area known as the Industrial Shop/Parking Area (see Figure 3.2). Much of the site is paved or covered by buildings.

Building 113 was used between 1955 and 1991 primarily for aircraft munitions systems and avionics maintenance, including some vapor degreasing operations. A 1,200 gallon concrete underground storage tank (UST) was located near the northeastern corner of Building 113. The UST received waste trichloroethylene (TCE) from degreasing operations conducted inside Building 113 from 1956 to 1968. Sometime after 1977, use of the UST was discontinued and it was filled with sand. In 1988, the UST was excavated and removed, and an underground discharge pipe associated with the UST was discovered. TCE has been detected in monitoring wells at concentrations ranging from six to 11,000 μg/L, which is many times TCE's maximum contaminant level of 5 μg/L. The soil and groundwater contamination at this site is believed to be primarily a result of the historic use of the TCE tank and associated overflow pipe (MWH, 2004).

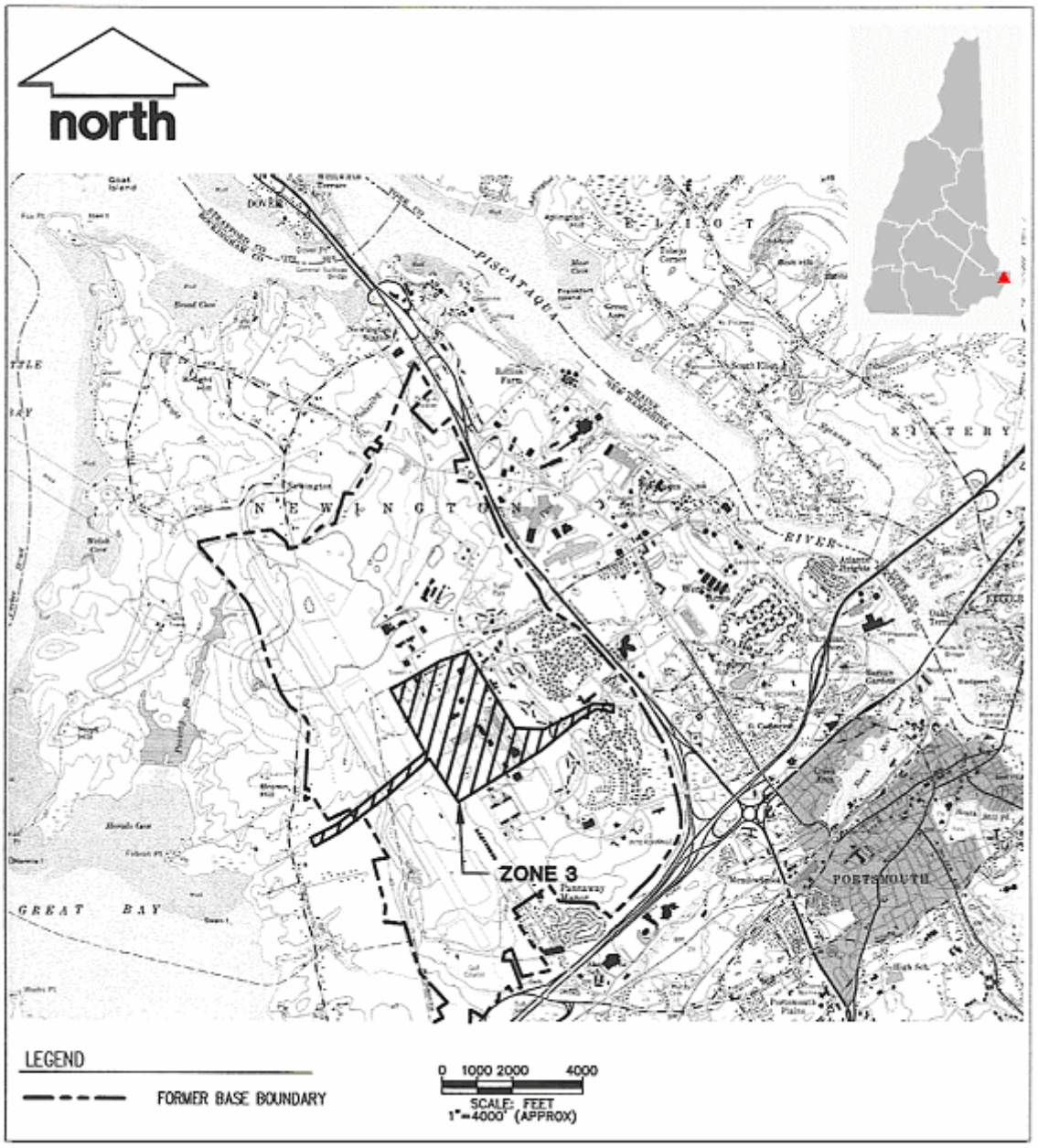

Figure 3.1: Pease AFB site location map (From MWH, 2004)

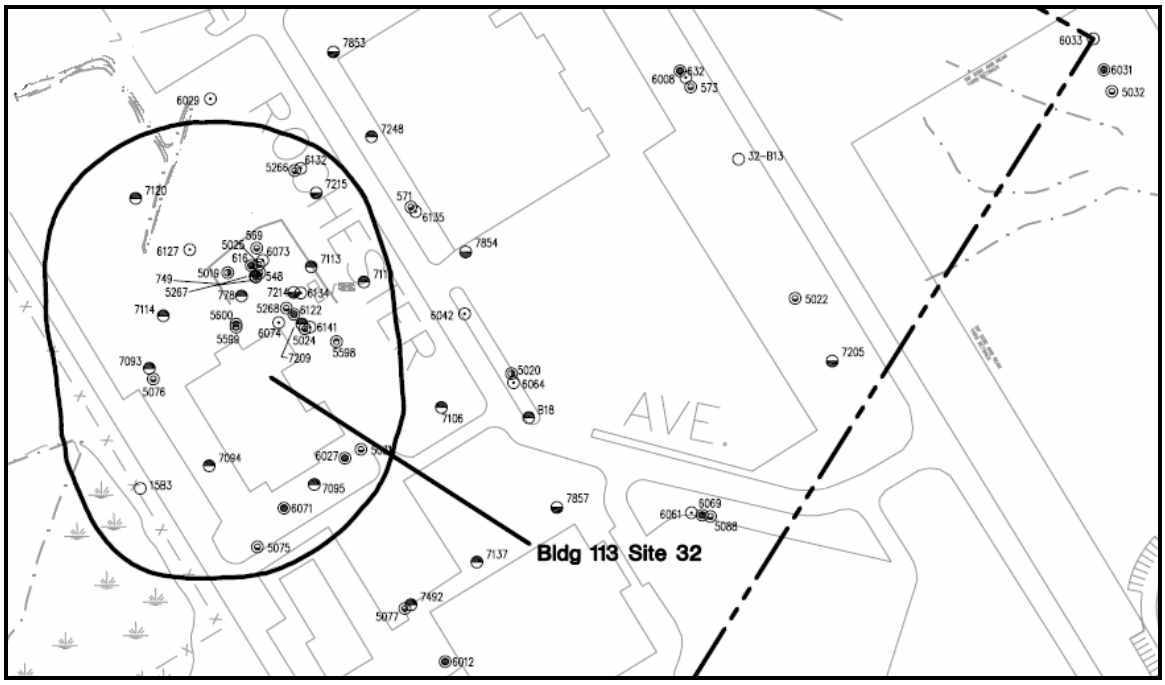

Figure 3.2: Site 32 location map (From MWH, 2004)

Monitoring well data at site 32 show the contaminant plume has traveled several hundred feet (See Figure 3.3). Previous studies (MWH, 2004) indicate the overburden in the vicinity of the site is approximately 20 to 30 feet thick and consists of fine grained marine silt and clay. Bedrock below the overburden consists of crystalline sedimentary and igneous rock with a pervasive fracture network.

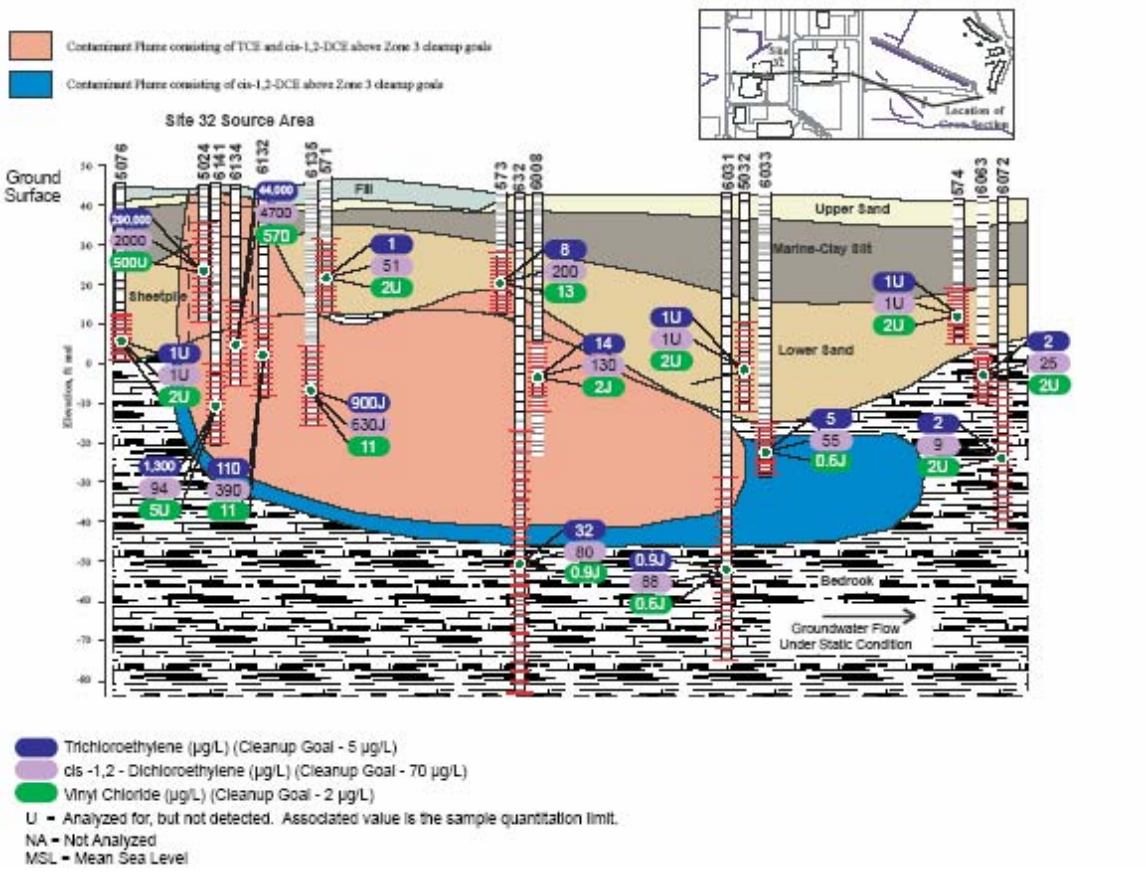

Figure 3.3: Cross Section of Site 32 Plume (MWH, 2004)

3.3 Model Selection

A numerical model is required to simulate the relatively complex fractured system at Pease AFB Site 32. Previous thesis research (Staples, 2002) has shown that an EPM model is appropriate for use in simulating contaminated fractured media, so long as the scope of the simulation problem is large compared to the scale of the fractures (Lee and Lee, 1999). Other studies have also shown that EPM approaches are appropriate for simulating fractured systems (NRC, 1990; EPA, 2001).

A true DFN or dual-porosity model would need significantly more site data to characterize the fractures. In addition, DFN models are limited to near-field scales (50-

100 m) due to the large computational demands of these models (Painter and Cvetkovic, 2005). However, FracWorks XP for MODFLOW can generate a detailed fracture network using data gathered from borehole logs and pump tests and export the information for use in MODFLOW (Dershowitz *et al.*, 2004). Based on the input from FracWorks XP, MODFLOW assigns values of hydraulic conductivity to cells in the MODFLOW grid. With these values, MODFLOW is able to simulate the heterogeneity and anisotropy of the fractured system. This approach using FracWorks XP has been successfully applied in carbonate, fractured till, crystalline, and clastic systems (Dershowitz *et al.*, 2004). The geology of fractured, crystalline rock is somewhat similar to these systems, and, as such, the hybrid DFN/EPM approach is considered appropriate for modeling the fractured system at Pease AFB. In addition, FracWorks XP is readily accessible by the author, with technical support available. Therefore, FracWorks XP for MODFLOW was selected for application to the problem.

3.4 Applying Hybrid DFN/EPM Approach to Construct Model of a Fractured Site

In this section, we discuss the method used to construct a MODFLOW-based EPM model using input from FracWorks. Clark (2004) provided step-by-step instructions for applying the DFN/EPM approach to build a model, which are summarized within this section. The programs used for this research include:

- FracWorks XP for MODFLOW (Version 4.10, supplied by Golder Associates)
- StrataFrac XP for MODFLOW (Version 4.10, supplied by Golder Associates)
- GMS 5.0 (supplied by DoD)

3.4.1 Input File Creation

The process begins with the creation of a 3-D fracture network and fracture file (.fab) using FracWorks XP. The site grid is created based on the conceptual model of the site (see Section 3.5). After creation of the grid, a fracture network (see Figure 3.4) must be created within the grid. In section 2.3.6, it was discussed that FracWorks XP idealizes fractures as planar polygons because they are computationally efficient and typically few field data are available to describe non-planar fractures (Dershowitz *et al.*, 2004). The varying colors displayed in Figure 3.4 relate to hydraulic conductivity values with darker shading representing lower conductivity fractures. The size of the polygons relates to the size of the fracture.

To create the network, average values for transmissivity, storativity, and fracture aperture (see section 3.5) were input into FracWorks XP. After creation of the fracture network, a finite difference grid of the same dimensions and units as those used in the fracture file will then be created in GMS. This will create a grid discretization file (.dis) which is necessary for use by StrataFrac XP (Clark, 2004). The discretization file must be converted into the format used by StrataFrac XP. It is essential to follow the required format to ensure StrataFrac XP is using units consistent with those in the GMS grid.

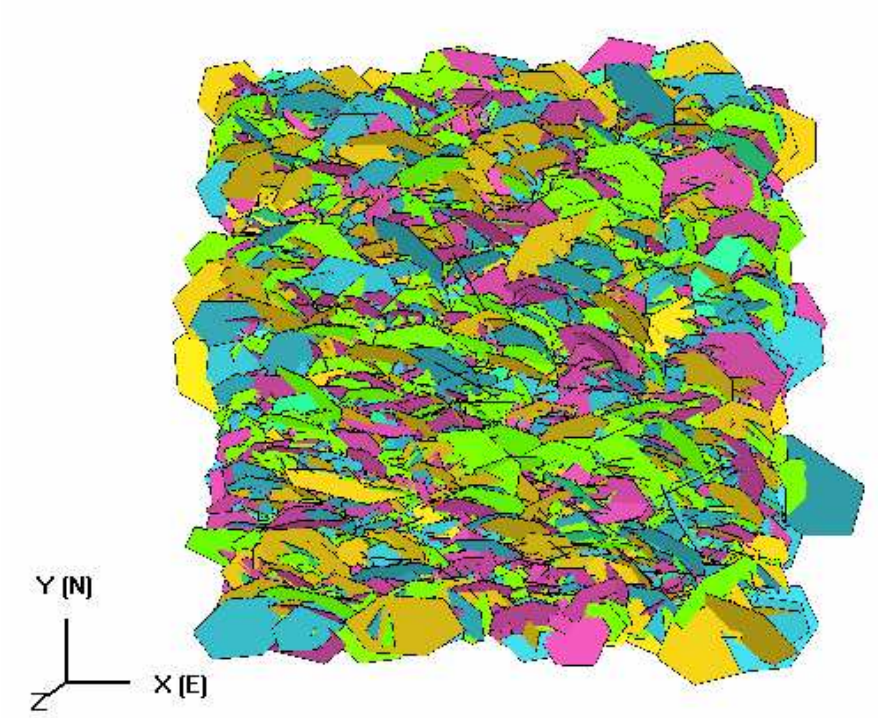

Figure 3.4: Fracture network created with Fracworks XP

3.4.2 StrataFrac XP Execution

Both the fracture file (.fab) and the GMS grid discretization file (.dis) are then imported into StrataFrac XP. Figure 3.5 shows the GMS grid being placed into the fracture network. Following the insertion of the GMS grid onto the fracture network, the Oda (1985) approach (see Section 2.3.6) was used to calculate EPM properties for grid cells based on the fracture properties within those cells. Essentially, the Oda approach integrates all the fractures contained within a grid cell and calculates an average value of hydraulic conductivity and porosity for that cell. The Oda analysis is performed within StrataFrac XP. The StrataFrac XP output can then be exported in GMS format (.dat). Two data files are created for use by GMS. The files contain hydraulic conductivity and porosity values for each cell in the grid. Should a cell contain no fractures, a zero value will result. GMS will not recognize zero values and they must be replaced with very

small, positive values for use in GMS (Clark, 2004). GMS is now ready to use the two files created by StrataFrac XP. We now have an EPM depiction of the fractured site, which can be used by GMS and was constructed using DFN data.

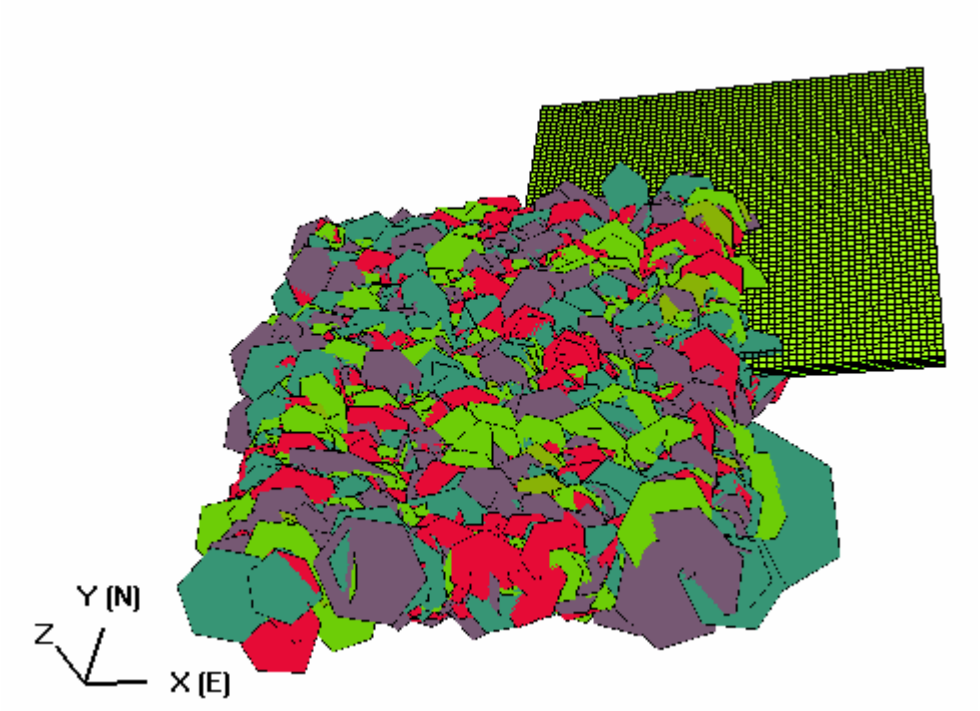

Figure 3.5: Convergence of EPM grid file with DFN fracture network

3.4.3 Assumptions

1) Steady-State Flow: This study will focus on long term containment of a chlorinated solvent plume. As is typical (Bakker and Strack, 1996; Charbeneau, 2000), steady state flow for the site was assumed since the time-scale of transient fluctuations in flow is large compared to the time-scale of the contaminant transport.

2) Sorption: Freeze and Cherry (1979) defined a retardation factor based on specific surface area of the fractures. Since there is very little data characterizing the geochemistry of the fractures, a retardation factor cannot be calculated based on the

Freeze and Cherry (1979) model. In addition, little attention has been placed on the analysis of sorption in fractured systems, and, as such, a simple retardation factor is generally assumed for sorption when modeling transport in fractured media (Berkowitz, 2002). Previous modeling efforts at this site have used a retardation factor of 1.8 to simulate adsorption of the TCE to the surrounding matrix, and as such, the same factor is assumed for this system (AFBCA, 1995).

3) Biodegradation: Natural attenuation relies on naturally occurring physical, chemical, and biological processes to control the migration of contaminants dissolved in groundwater (Bedient *et al.*, 1999). The Office of Solid Waste and Emergency Response (OSWER) states that "the hydrogeologic and geochemical conditions favoring significant biodegradation of chlorinated solvents sufficient to achieve remediation objectives within a reasonable timeframe are anticipated to occur only in limited circumstances" (OSWER Directive 9200.4-17P, 1999). In a fractured aquifer system with extreme heterogeneity and difficult monitoring conditions, natural attenuation of chlorinated solvents would be an infeasible remediation strategy. Based on this information, a conservative approach is taken, and the effects of biodegradation are assumed negligible.

3.5 Site and Remediation Model

In this section, a simple model of TCE contamination at Pease AFB is constructed. Model parameters, detailed assumptions, and model verification are explained.

3.5.1 Model Parameters and Detailed Assumptions

Contamination has primarily migrated into the bedrock (see Figure 3.3). To simulate flow and transport in the saturated zone, a MODFLOW finite difference grid was constructed that is 60 cells long by 60 cells wide by 4 cells deep, so that each cell is 10 meters long, 10 meters wide, and 5 meters deep. The following parameters and assumptions were used in the creation of the model:

1) Transmissivity and Storativity: These values are necessary for creation of the fracture network in FracWorks XP for MODFLOW. In the region of interest (Figure 3.2), the Air Force Base Conversion Agency (AFBCA) (1994) performed several pump tests and the largest value was used as input values for both transmissivity and storativity (see Table 3.1). The largest value was used because FracWorks XP only wants a single value. Based on the pump test data, the input values for both transmissivity and storativity were determine to be 53.05 m^2/d and 1.20 x 10^{-3} respectively.

Observation Well ID	32-6007	32-6014	32-6029	32-6033	32-6042
Transmissivity (m^2/d)	49.24	16.82	53.05	21.18	22.95
Storativity	5.14 x 10^{-4}	7.84 x 10^{-5}	1.20 x 10^{-3}	1.8 x 10^{-4}	1.97 x 10^{-4}

Table 3.1: Pump test results for Pease AFB (From AFBCA, 1994)

2) Fracture Density: This value is necessary for creation of the fracture network in FracWorks XP. Fracture densities observed in outcrops and cores from Site 32 over five to 15-foot intervals range from 0.07 to 4.0 fractures per foot (AFBCA, 1994). For a more conservative approach, the larger value of 4.0 was used in the creation of the fracture network.

3) Constant Head Boundaries: Since the model assumes steady state flow conditions, constant head boundaries are defined to induce flow through the site. Figure 3.6 shows the potentiometric surface of the site and was used to determine the west and east boundary conditions for the model. The constant head boundary for the western edge of the model is 51 ft (15.55 m) mean sea level (msl) and the boundary for the eastern edge is 47 ft (14.33 m) msl.

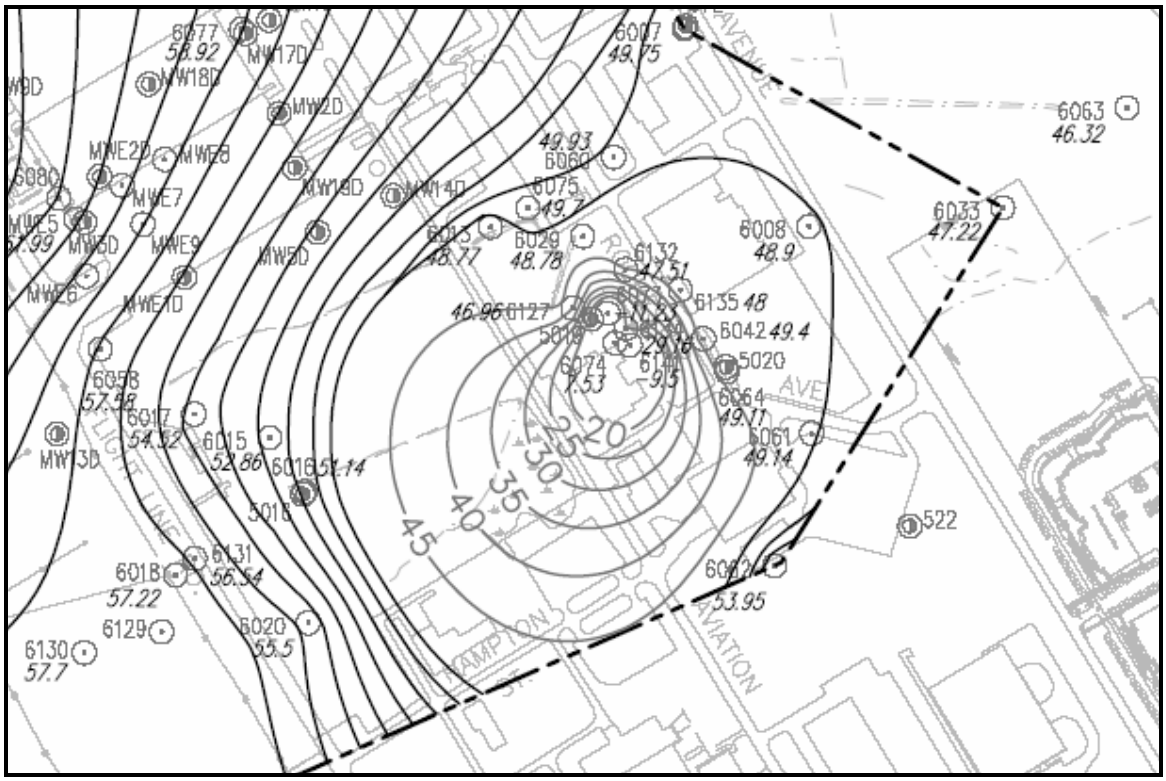

Figure 3.6: Site 32 potentiometric surface in ft MSL (From MWH, 2004)

4) Anisotropy: The differing values of vertical and horizontal hydraulic conductivity refer to the anisotropy of the system. Generally, anisotropy of up to two orders of magnitude is found in fractured media (Domenico and Schwartz, 1998). FracWorks XP for MODFLOW calculates both vertical and horizontal hydraulic conductivity for each

model cell using the Oda approach. The ratio of these values is input into GMS as the anisotropy values for the system. As a result, there is no need to assume a single anisotropy value for the system.

5) Plume Generation: Only TCE was considered in the study. The plume was generated under the assumption that the contaminant source covered the full depth (20 m) of the bedrock. The source area is shown in Figure 3.7. Table 3.2 shows maximum TCE values detected in the source area wells. Each well was considered a source and these concentrations were assumed constant in time. Each of the values in Table 3.2 was placed in the GMS grid based on actual location of the corresponding well within the grid. The model was run allowing the natural gradient of the system to distribute the contaminant plume.

Observation Well ID	32-5024	32-6014	32-6073	32-6074
Max TCE (mg/L)	930	110	34	940

Table 3.2: Maximum TCE values in source area (From MWH, 2004)

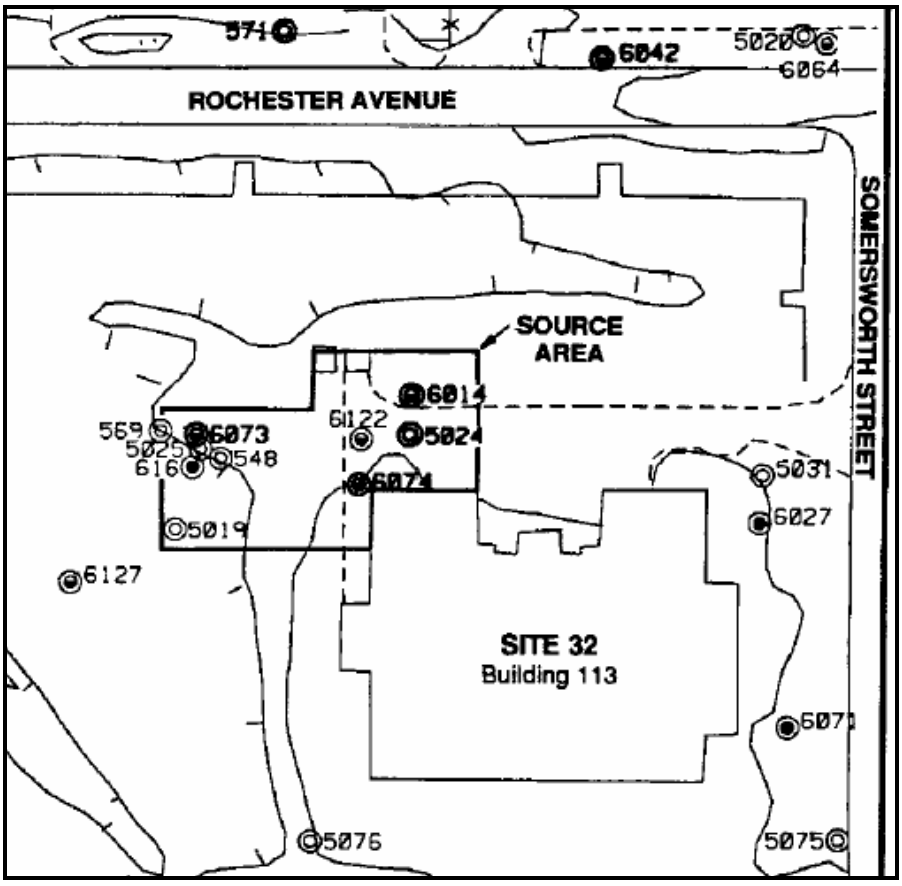

Figure 3.7: Site 32 source area (From AFBCA, 1995)

3.5.2 Model Validation

After creation of the model using the above input parameters, the model was evaluated. In section 2.4, a method was proposed to assist in the model validation process. This provided a basis for the validation process. Initially, monitoring well locations within the model were placed according to actual locations shown in Figure 3.3. Historical head and contaminant data were available for these wells, and allowed for comparison of actual observed values with the model calculated values.

After construction, model-derived values of hydraulic conductivity were examined to see how they compared to conductivities calculated for the site using

traditional pump test interpretation techniques. First, StrataFrac XP calculated hydraulic conductivity values for each cell in the GMS grid. These values were compared with pump test results. Several pumping tests were conducted at Site 32 and were used to determine the average horizontal hydraulic conductivity value to be 4.5 m/d (AFBCA, 1995). Values calculated using StratFrac XP ranged from 0 to 17 m/d (see Appendix C) with the vast majority of values in the range of 4 to 8 m/d. The average vertical hydraulic conductivity value was determined to be 2.5 m/d (AFBCA, 1995). Values calculated using StrataFrac XP ranged from 0 to 11 m/d with the vast majority of values residing in the range of 2 to 3 m/d. Based upon observed site data and model data, the FracMan XP software appears to accurately calculate hydraulic conductivity values for the system.

The next step involved comparison of measured and modeled heads. Head values were taken from observed water level readings at several monitoring wells. Monitoring wells representing the actual wells (shown in Table 3.3 and Figure 3.2) were placed in the model grid to allow for comparison of head values. Table 3.3 provides a summary of the model's ability to match simulated heads with actual heads. This table lists the eight wells used to evaluate how well the flow model simulated actual conditions. The table also presents the residual, or difference, between simulated and observed values. The relative root mean squared error ($RMSE_r$) between measured and modeled water levels is 0.013. The $RMSE_r$ normalizes the mean square error by dividing through by the mean observed value. The small $RMSE_r$ indicates the modeled values adequately match the observed values.

Well ID	Observed Water Level (m MSL)	Model Head (m MSL)	Model Residual (m MSL)	Residual^2 (m^2 MSL)
32-5020	14.94	14.85	-0.09	0.0081
32-5022	14.48	14.44	-0.04	0.0016
32-5024	15.06	15.01	-0.05	0.0025
32-5076	15.14	15.1	-0.04	0.0016
32-6008	14.67	14.61	-0.06	0.0036
32-6029	14.88	15.25	0.37	0.1369
32-6033	14.58	14.2	-0.38	0.1444
32-6074	15.08	15.02	-0.06	0.0036
				0.3023
	Root Mean Squared Error			0.19439
	Relative RMSE			0.013087

Table 3.3: Simulated versus actual head values

The next step involved comparing simulated contaminant concentrations with observed values at the same eight wells. With only the natural gradient forcing flow through the system (*i.e.*, no pumping), the actual contaminant concentrations (see Appendix A) were to be compared with simulated contaminant concentrations. It was discovered during this phase of model validation that the model required extensive computational effort to simulate transport. GMS required over three hours to simulate one year of transport, with the simulation time increasing exponentially for times greater than one year. For example, the model was run for three full days to simulate 585 days of transport. Data are available at the actual site from 1992 until 2003 (see Appendix A), but the computational effort required by GMS would not allow for a simulation spanning those 11 years.

A possible reason for this lies in the fact that FracMan outputs a porosity value for each cell in the GMS model grid. A simulation was run after specifying a single porosity value for all cells, and the one year simulation was completed in a little over one hour

(three times faster than when each cell has its own porosity specified). It appears this may be a limiting factor of implementing the DFN/EPM approach in GMS.

Monitoring data for Pease AFB are available from 1992 to 2003 (see Appendix A), but the initial time that the contamination source was released (t = 0) is unknown. Therefore, the contaminant plume was developed using the concentration data shown in Section 3.5.1 as the initial condition in 1992 (t = 0). The model was set to run from t = 0 until December 1996. This signifies the last measurement before Pease AFB implemented a pump-and-treat system at the site. As discussed above, the model took three full days to run 585 days of transport. Figure 3.8 compares the actual plume in December 1996 and the model plume simulated assuming the hydrogeological conditions described in section 3.5.1. The actual plume was generated by kriging the December 1996 concentrations tabulated in Appendix A. Inspection of the actual plume (Figure 3.8a) shows the contamination appears to be moving in a northeastern direction. The model plume (Figure 3.8b), although only showing 585 days of data, also shows the plume moving in a northeastern direction. Although the GMS model was unable to simulate the full four years (1992 to 1996) of data, it appears that it does adequately model the direction of transport and replicates the approximate size and shape of the plume.

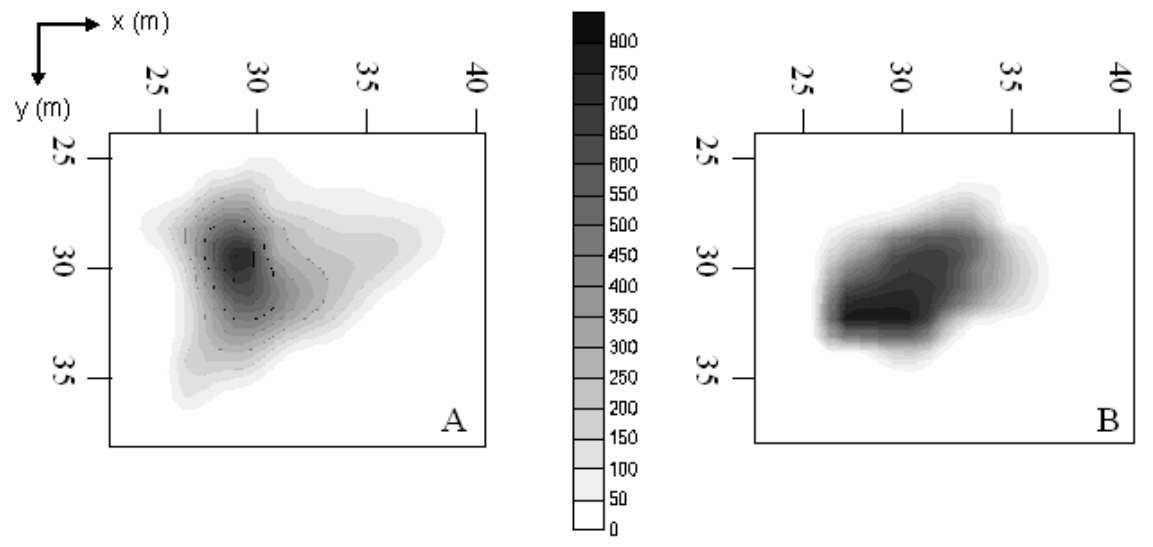

Figure 3.8: Comparison of (A) actual (December 1996) versus (B) simulated plume

3.6 Model Analysis

After gaining confidence that the model was running properly, an analysis of the model was conducted to answer the research question of whether the hybrid DFN/EPM approach can be used to manage contaminated fractured media sites. It was concluded that complete groundwater restoration to applicable or relevant and appropriate requirements (ARARs) at Site 32, in a reasonable time frame, was not feasible under any remedial scenario (MWH, 2004). As such, the recommendation was to isolate the source area to prevent continued migration of contaminated groundwater. An actual pump-and-treat system was installed at Site 32 in 1997, and this system will be used to compare with the model predictions of pump-and-treat performance. A plume was built in GMS (see Figure 3.8a) by kriging the December 1996 monitoring data (see Appendix A) to examine placement and pumping options of a pump-and-treat system. These concentration values served as the initial time (t = 0) for all simulations. Wells were

placed at various locations (see Figure 3.9) within the source area and around the toe of the plume based on their actual location at the site.

Various pumping scenarios were simulated to find the optimal configuration of wells to effectively contain the contaminant plume. All pumping scenarios were simulated under steady state flow conditions. The layer of clay and silt overlaying the bedrock unit is the limiting factor on pump rates. WESTON (1993) evaluated the site and determined the maximum allowable pump rate for Site 32 is 15 gpm (0.06 m^3/min). Pump rates above this will result in excessive consolidation of the overburden and cause the ground surface to subside and settlement of buildings in site 32 (AFBCA, 1994).

Table 3.4 summarizes the four scenarios simulated with the model. The first scenario simulated the effects of the hydraulic gradient only. No pumps were operational in this scenario. The second scenario simulated the actual operating pump-and-treat system with four source wells pumping at the maximum allowable pump rate. The third pumping scenario was simulated with only two wells pumping at the toe of the existing plume. The fourth scenario was simulated with both the four source wells and the two toe wells in operation. Figure 3.9 shows the locations of the pumping wells, as well as

Parameter	**Pumping Scenario**			
	1	**2**	**3**	**4**
Number of Pumping Wells	0	4	2	6
Total Pumping Rate (gpm)	15	15	15	15
Total Pumping Rate (m^3/d)	82	82	82	82

Table 3.4: Model parameters

the locations of downgradient monitoring wells. Well numbers 32-5024, 5268, 6074, and 6134 are the source wells. Well numbers 32-5020 and 7854 are the toe wells. Well numbers 32-5022, 6008, and 6033 are the downgradient monitoring wells.

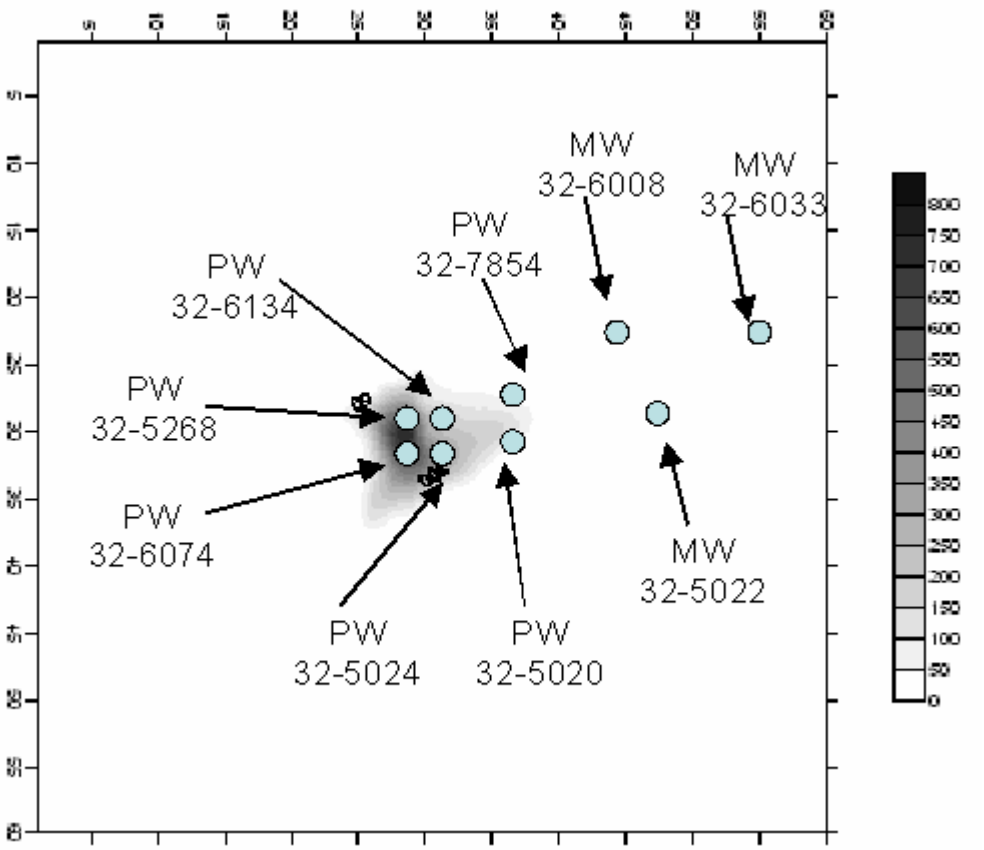

Figure 3.9: Pumping (PW) and monitoring (MW) well locations

To measure the effectiveness of the pump-and-treat system, simulated concentration data will be compared with actual monitoring data while the system is operating and not operating. Within the GMS model, observation points (monitoring wells) were placed at the same location as the pumping wells. The comparisons will help answer the research question of how the model can be used to manage contaminated fractured media sites. Results are summarized in Chapter 4.

4 Results and Analysis

4.1 Overview

In this chapter, the data gathered from the model described in Chapter 3 is analyzed to answer the research questions: what is the confidence of the ability of the model to "adequately" simulate transport in fractured media and how might the model be used to manage contaminated fractured sites. In Chapter 3 we discussed that a limiting factor of this model lies in the computational effort needed to simulate transport. Due to this limitation, we only were able to conduct one-year simulations at the site. The existing pump-and-treat system was put in service in 1997, and the model performance was evaluated using the data from 1997 to 1998 (see Appendix A).

4.2 Model Results and Analysis

This section will discuss model performance based on the results of the pumping scenarios. Table 4.1 summarizes the parameters used for each pumping scenario. As a reminder, scenario one is simulating the action of the plume with no wells in operation. Scenario two is simulating four wells in the source zone. Scenario three is simulating two wells 38 meters (125 feet) downgradient from the source at the toe of the plume. Scenario four is simulating all six wells in operation. Figure 4.1 shows all well locations for the scenarios.

Parameter	Pumping Scenario			
	1	2	3	4
Number of Pumping Wells	0	4	2	6
Total Pumping Rate (gpm)	15	15	15	15
Total Pumping Rate (m^3/d)	82	82	82	82

Table 4.1: Model parameters

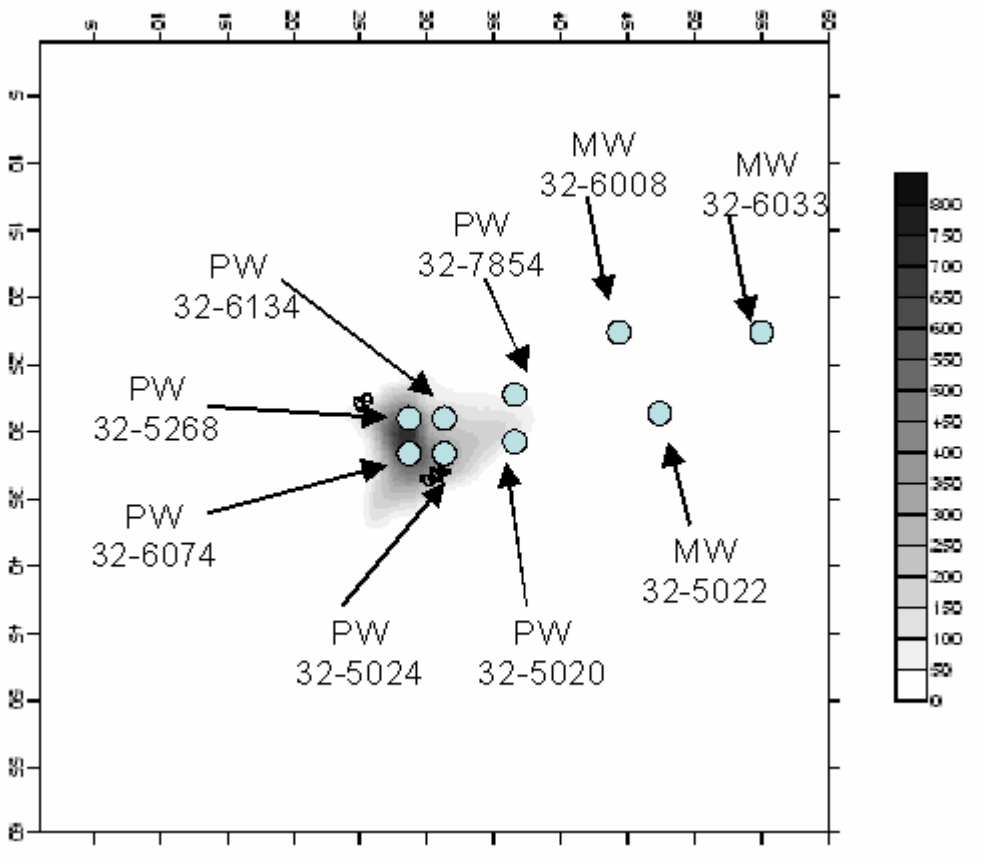

Figure 4.1: Pumping (PW) and monitoring (MW) well locations

Heads at the site were simulated for each pumping scenario. The minimum allowable water elevation, based on previous geotechnical evaluations (AFBCA, 1994), was determined to be 12.8 meters (42 feet). The head simulations indicated that drawdown was within allowable limits for all pumping scenarios.

4.2.1 Pumping Scenario One

Scenario one simulates the effect of only the hydraulic gradient (i.e., no pumping) on the movement of the contaminant. The simulation was run for one year and its output offers a baseline for future scenarios. Figure 4.2 shows the contaminant plumes before (A) and after (B) one year's time. Figure 4.2a is based on the last actual concentration measurements taken before 1 January 1997. The figure shows the plume migrating slowly to the northeast (with north being toward the top of the page), as expected. From Section 3.5.1, recall the hydraulic conductivity at the site averages 4.5 m/d. Thus, unless the hydraulic gradient is quite large, it would be anticipated that the plume would not migrate far from the source within one year. Figure 4.3 shows a graphical representation of simulated concentration data at the pumping wells. Figure 4.4 depicts the simulated concentration data at the downgradient monitoring wells.

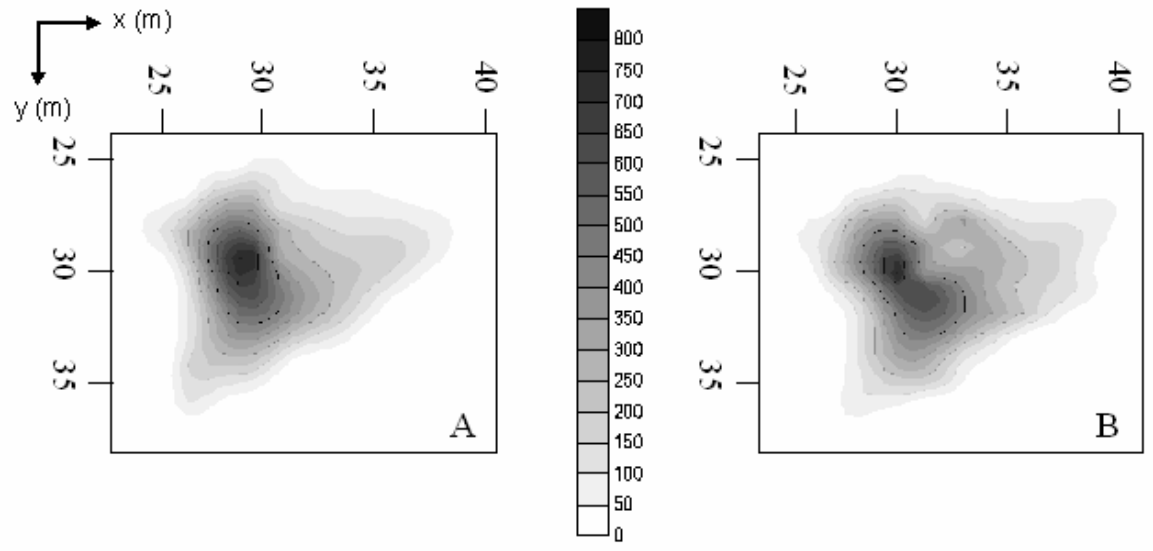

Figure 4.2: Simulated plume at (A) t = 0 and (B) t = 1 year for scenario one

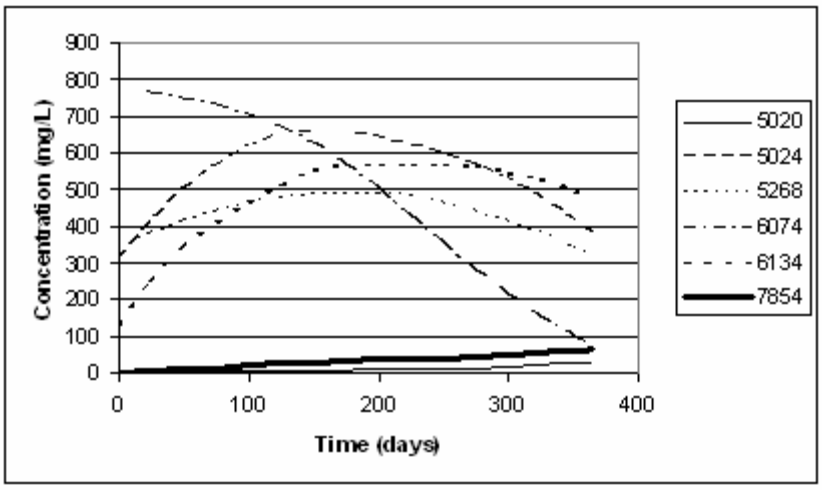

Figure 4.3: Simulated TCE concentrations at pumping wells for scenario one

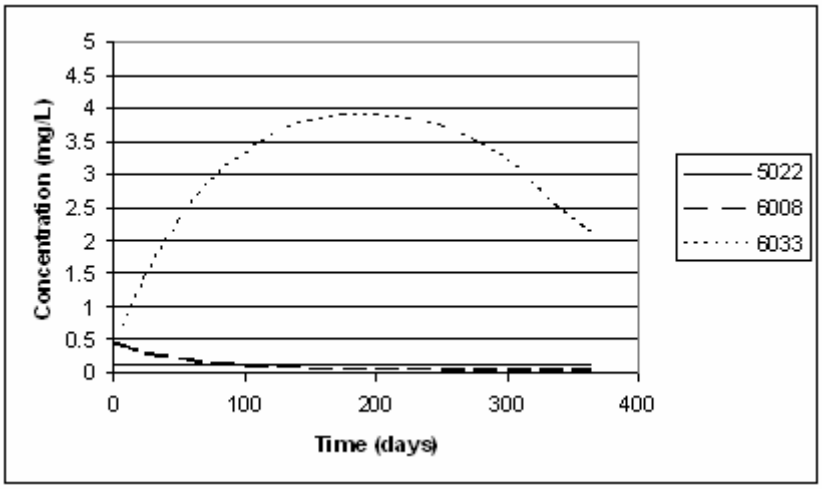

Figure 4.4: Simulated TCE concentrations at downgradient monitoring wells for scenario one

Figure 4.3 shows that without any pumping, the TCE concentrations will remain well above the MCL of 5 μg/L at all wells (see Table 4.2). Downgradient wells shown in Figure 4.4 depict TCE levels above the MCL, but at much lower concentrations, suggesting the TCE is migrating very slowly from the source area.

4.2.2 Pumping Scenario Two

Scenario two simulates the actual pump-and-treat system installed at Site 32 in 1997. The simulation was run for one year and comparisons were made with actual monitoring data at the site. In this simulation, only the four source pumping wells (5024, 5268, 6074, and 6134) were operating. Figure 4.5 compares the simulated contaminant plume after one year of natural gradient transport (A) with the plume that is simulated with the pumping wells in scenario two (B). The figure shows the model simulating the expected behavior, with the source area contained, but negligible effects on the toe of the plume within the one year simulation period.

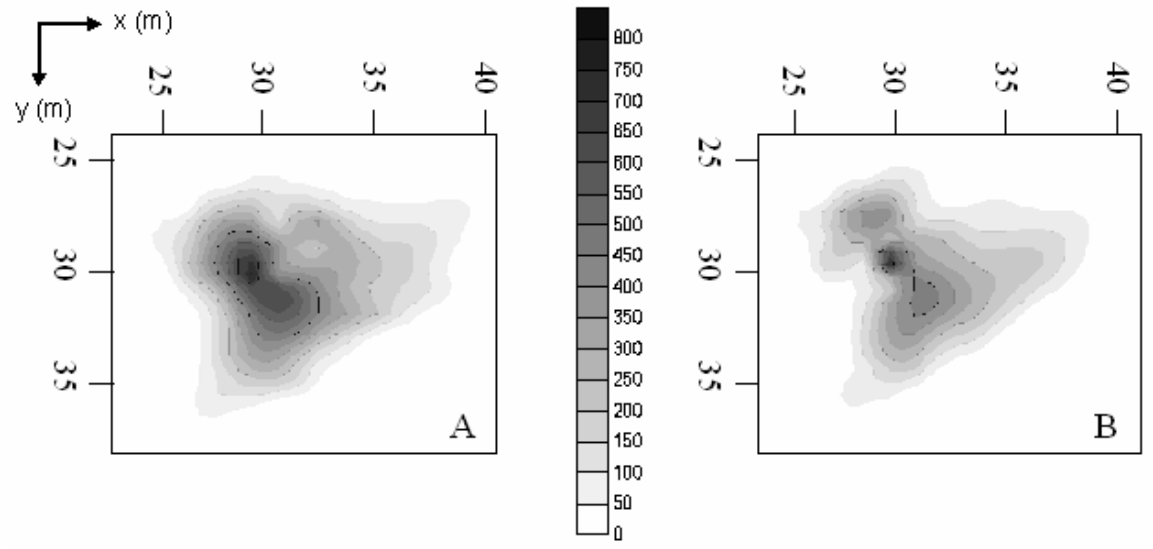

Figure 4.5: Comparison of simulated plumes after one year of (A) natural gradient transport and (B) implementation of pumping scenario two

Figure 4.6 shows the simulated and actual monitoring data at the four pumping wells for calendar year 1997. Comparison of the simulated and actual values show the model does a reasonable job of simulating the actual pump-and-treat system.

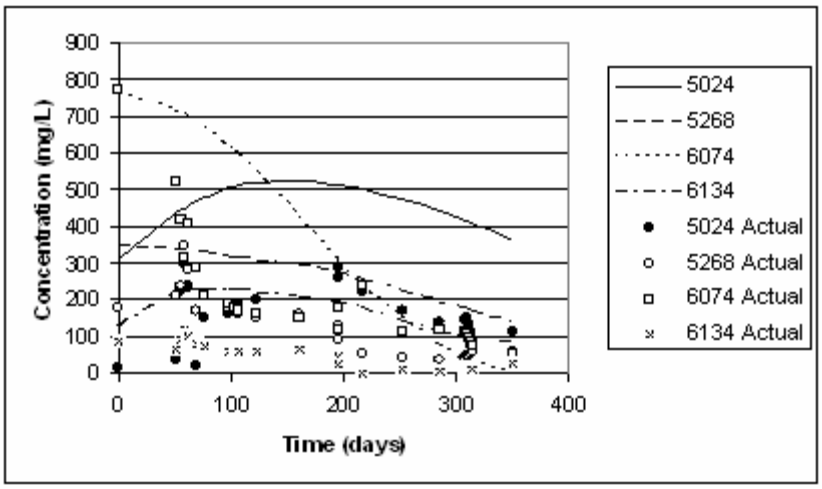

Figure 4.6: Simulated and measured TCE concentrations for pumping scenario two at four source wells

Figure 4.7 shows simulated and measured TCE concentrations for the two monitoring wells at the toe of the plume. We see that the simulated concentrations overestimate the measured values, which is not unexpected given the aquifer's heterogeneity and the fact that the model has not been calibrated to the data.

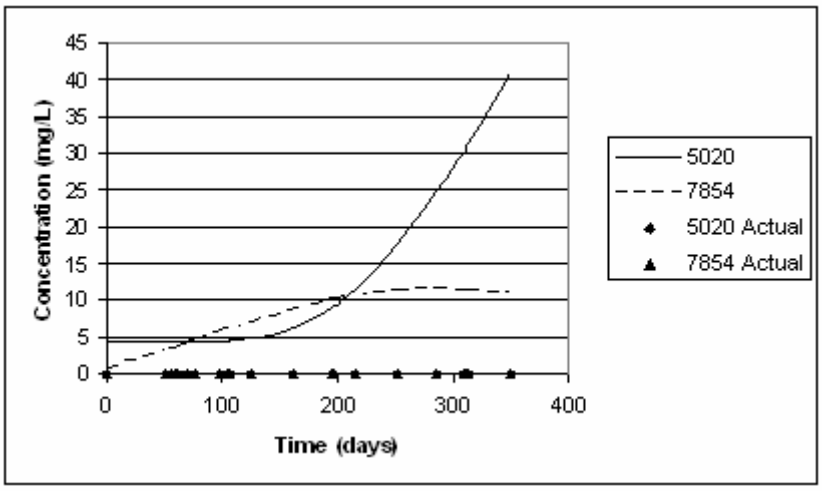

Figure 4.7: Simulated and measured TCE concentrations for pumping scenario two at two toe wells

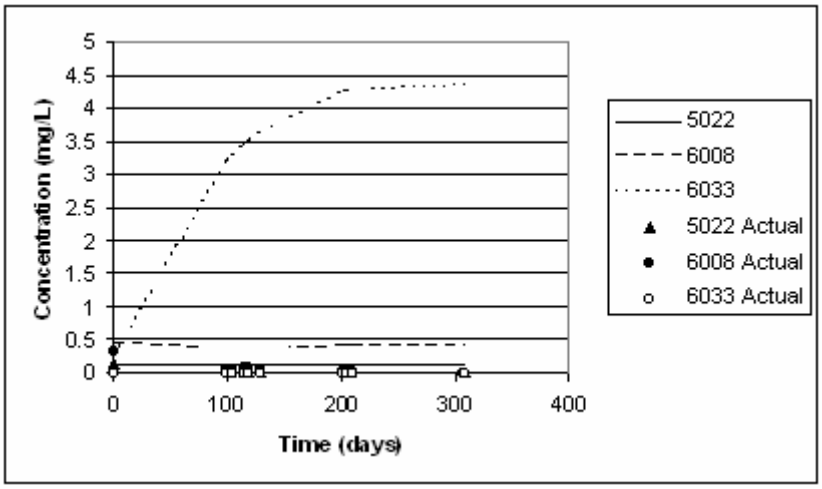

Figure 4.8: Simulated and measured TCE concentrations for pumping scenario two at three downgradient wells

Figure 4.8 shows simulated and measured TCE concentrations for the three far downgradient monitoring wells. TCE concentrations at the downgradient wells (measured and simulated) are above the MCL, but at much lower concentrations than at the wells closer to the source. This suggests the TCE is migrating very slowly.

4.2.3 Pumping Scenario Three

Scenario three involved using two pumping wells (5020 and 7854) placed at the toe of the plume. Figure 4.9 compares the simulated contaminant plume after one year of natural gradient transport (A) with the plume that is simulated with the pumping wells in scenario three (B). As expected, the plume migrates toward the two wells, but there is limited effect on the source zone. It appears that the pumps would effectively contain the plume from further migration downgradient, but would have negligible effect on the source.

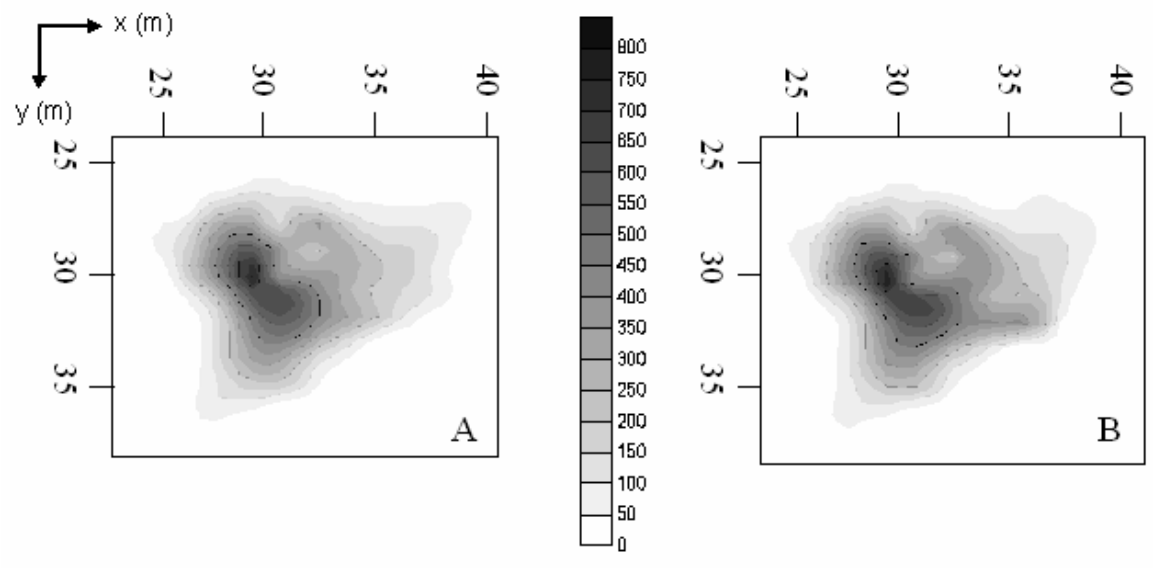

Figure 4.9: Comparison of simulated plumes after one year of (A) natural gradient transport and (B) implementation of pumping scenario three

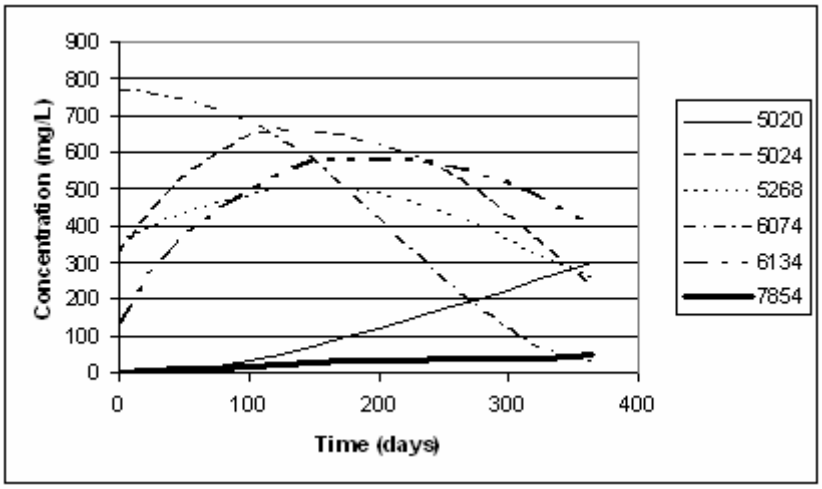

Figure 4.10: Simulated TCE concentrations at pumping wells for scenario three

Figure 4.10 shows modeled TCE concentrations at each of the pumping wells. As expected, concentrations rise in the two pumping wells that are operational in scenario three (5020 and 7854) as plume capture is achieved. Comparing Figures 4.3 (no pumping) and 4.10 (scenario three), we see that the impact of scenario three on

concentrations at the pumping wells is minimal. Figure 4.11 shows simulated TCE concentrations at the downgradient monitoring wells for scenario three. Comparison with Figure 4.4 shows that at least in the one-year time frame of the simulation, pumping wells at the plume toe do not greatly affect concentrations at the downgradient monitoring wells. Concentrations at the downgradient wells remain above the MCL for TCE.

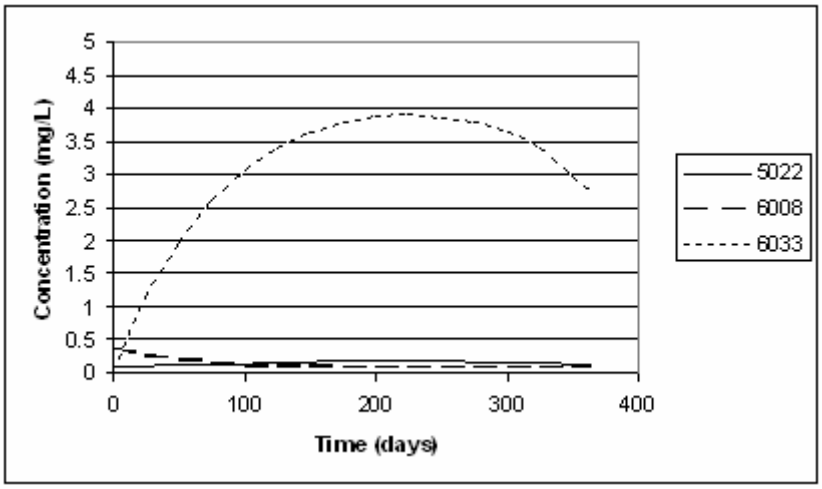

Figure 4.11: Simulated TCE concentrations at downgradient monitoring wells for scenario three

4.2.4 Pumping Scenario Four

Scenario four involved all six pumping wells operating. Figure 4.12 compares the simulated contaminant plume after one year of natural gradient transport (A) with the plume that is simulated with the six pumping wells in scenario four operating (B). As expected, the four source wells (5024, 5268, 6074, and 6134) were effective at containing the source area. In addition, the toe of the plume appears to migrate toward the wells placed at the toe (5020 and 7854).

Figure 4.13 displays the simulated TCE concentrations for scenario four at the six pumping wells. As expected, with all six pumps operational, the source area

contamination is being contained and TCE concentrations near the source zone are reduced.

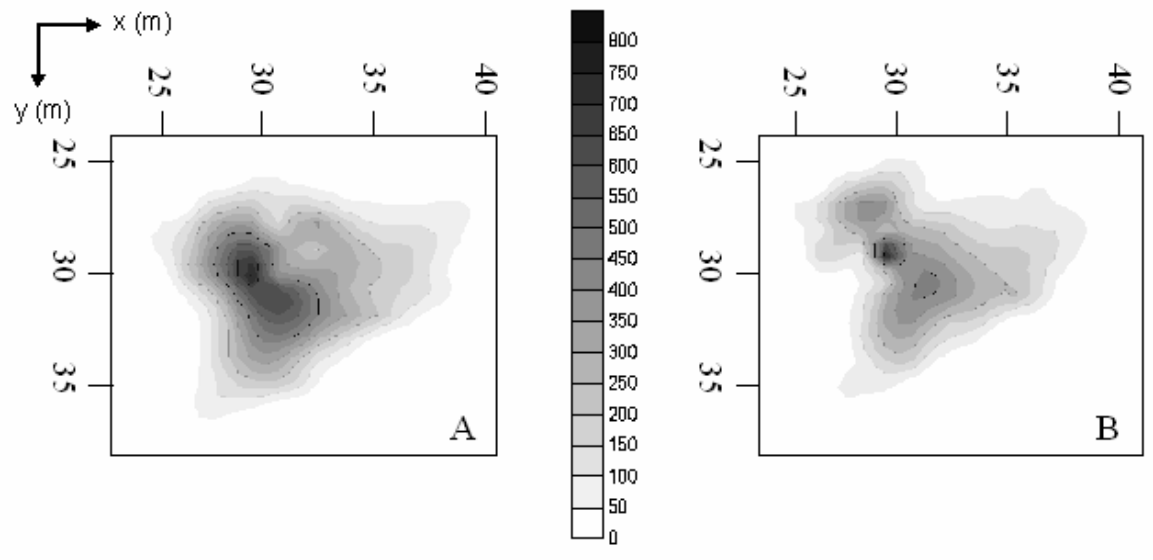

Figure 4.12: Comparison of simulated plumes after one year of (A) natural gradient transport and (B) implementation of pumping scenario four

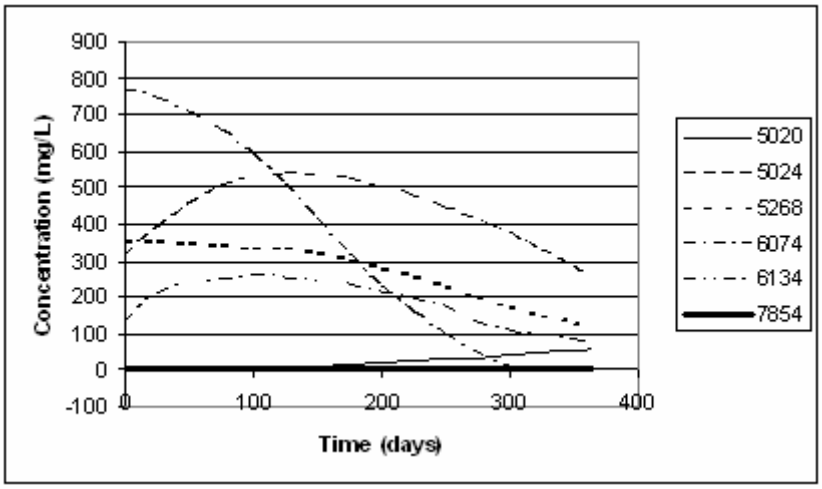

Figure 4.13: Simulated TCE concentrations at pumping wells for scenario four

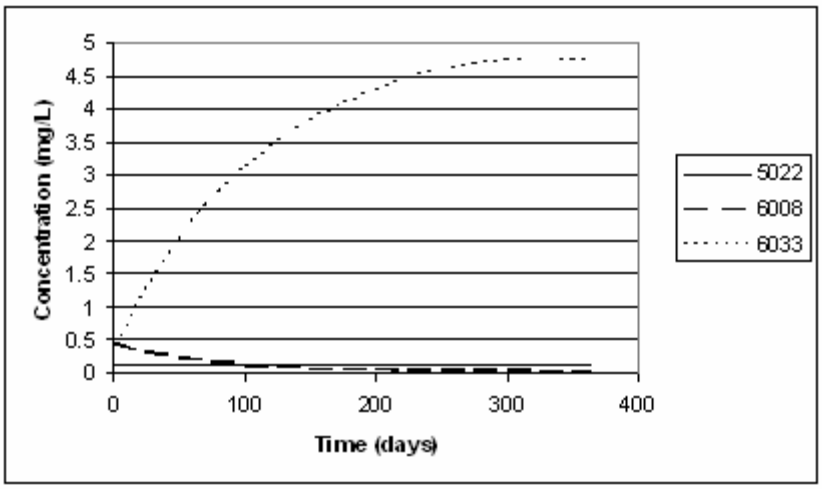

Figure 4.14: Simulated TCE concentrations at downgradient monitoring wells for scenario four

Figure 4.14 displays the simulated TCE concentrations at the three downgradient monitoring wells. Not unexpectedly, even with all six pumping wells in operation, the levels of TCE downgradient are unaffected within the one year simulation period.

4.3 Results Summary and Discussion

Table 4.2 compares the simulated TCE contaminant concentrations at each well for each scenario after the one year simulation. It also compares the concentrations simulated in scenario 2, which models the actual pump-and-treat site remediation, with measured concentrations after one year of pump-and-treat system operation. In all scenarios, the contaminant concentrations observed both at the source and downgradient wells failed to meet the MCL for TCE (5 μg/L). Although standards were not met, it can be noted that the modeled pumping system (scenario two) simulated the salient characteristics of the data obtained during operation of the actual pump-and-treat system (section 4.2.2).

Scenario	Source Wells				Toe Wells		Downgradient Wells		
	5024	5268	6074	6134	5020	5024	5022	6008	6033
1	379.22	322.37	75.65	478.51	27.45	62.48	0.128	0.017	2.118
Actual	110.00	58.00	51.00	28.00	0.017	0.004	0.004	0.006	0.008
2	339.47	127.79	0.278	74.44	44.89	10.82	0.127	0.398	3.947
3	230.80	256.87	29.61	405.00	302.35	49.47	0.132	0.068	2.737
4	257.59	118.43	0.041	74.23	55.79	3.65	0.127	0.008	4.695

Table 4.2: Simulated and measured TCE concentrations at all wells after one year for all model scenarios

Comparison of scenario one with the other scenarios allows us to evaluate the impact of pumping on contaminant transport. With the four source pumps operating (scenario two), we see a dramatic decrease in source zone concentration over the one year operation. With only the two toe wells operating (scenario three), we see less reduction in the source zone concentration, along with a concentration increase in the toe wells. This is to be expected, as the pumping toe wells are capturing contaminated water from upgradient. Looking at all six wells in operations (scenario four), we see that there is little difference from the scenario with only the four source wells pumping.

From examination of Table 4.2, it appears that scenario two would be the most effective at this site. Operation of only the toe pumps may contain the plume from further migration, but it fails to address the source zone. Additionally, operation of all six pumps has little added benefit from operating only the four source pumps.

Comparing the scenario two simulation with the measured concentrations, we see that the simulated concentrations are generally greater than the measured values. The fact that the simulations and measured values are different is not surprising, given the heterogeneity of the real system and the fact that the model has not been calibrated to the

data. The fact that the model generally overestimates the measured values may in part be due to the model assumption that biodegradation is negligible, when in reality, biodegradation may be an important process affecting the fate of the TCE plume.

The fact that the model simulated downgradient concentrations above MCL for all pumping scenarios can possibly be attributed to the short run time of the model or that the contaminant bypassed the capture zone of the pumping wells. It is noted that no optimization of the system was considered in this study.

5 Conclusions

5.1 Summary

The goal of this research is to ascertain if currently available models can be used as tools in managing groundwater contamination in fractured aquifers. A DFN/EPM model of an actual site was constructed based upon site geotechnical data (MWH, 2004) and previous modeling efforts (AFBCA, 1994) in an attempt to evaluate the practicability of using a hybrid DFN/EPM model to help decision makers manage groundwater contamination in fractured aquifer systems.

The evaluation was conducted using conditions found at a contaminated fractured aquifer at Pease Air Force Base, New Hampshire. A DFN/EPM model of the site was constructed and simulations run for various remediation scenarios, including a "no-action" scenario and a scenario that replicated the actual pump-and-treat system that was selected for the site. The simulations showed that the model reasonably simulated hydraulic and contaminant responses to remediation activities at the site, and that pump-and-treat systems have the potential to contain the plume, although contaminant levels were predicted to remain above MCLs, at least within a year of implementation of the remedial remedy.

5.2 Conclusions

Existing models are helpful in developing an understanding of the behavior of groundwater flow and contaminant transport in fractured aquifers. A review of the literature indicates that there are a wide range of models which incorporate many of the salient processes that impact flow and contaminant transport in fractured media. The

more complex models, which explicitly account for the effects of individual fractures on fluid flow and contaminant transport, require data that are typically unavailable at a remediation site.

The hybrid DFN/EPM model is appropriate for application in a fractured system. The literature suggests that an EPM model is appropriate when dealing with fractured rock in the absence of detailed site data as long as the scale of the system being modeled is sufficiently larger than the scale of fracturing. The literature also shows that it is appropriate to convert DFN data to equivalent data that can be used in an EPM model. In this study, we demonstrated that a hybrid DFN/EPM model could adequately simulate flow conditions at a fractured site. It was also seen that at least qualitatively, the model could be used to replicate the salient characteristics of field data obtained during a pump-and-treat remediation of a contaminated fractured aquifer.

Numerical modeling using the DFN/EPM can help decision makers manage contaminated fractured aquifers. Numerical modeling provides decision makers with a tool they can use to gain an understanding of flow and transport in a complex, heterogeneous, fractured system. The DFN/EPM uses multiple cells to represent varying hydraulic conductivities in order to simulate the impact of the heterogeneous conditions commonly associated with fractured aquifers on contaminant transport. With the DFN/EPM, the potential effects of alternative remedial actions on contaminant movement and fate can be simulated, in order to design and optimize remediation technologies. The numerical model built based on hydrogeologic data from Pease AFB provided a general understanding of how a pump-and-treat system could be applied in a fractured rock aquifer at Pease AFB. Model analysis indicates pump-and-treat

technology may be appropriate for containing contaminant plumes under the hydrogeologic conditions encountered at Pease AFB, though cost and cleanup times may exceed acceptable limits. As shown in this study, contaminant levels were reduced with the installation of the pump-and-treat system; however, it was also noted that none of the scenarios simulated resulted in contaminant levels achieving MCLs.

5.3 Recommendations

Explore the use of newer and faster computers with the hybrid DFN/EPM model to simulate the transport of contaminants in fractured aquifers. As noted in Chapters 3 and 4, the computational effort necessary to run this model was much more than that needed to run an EPM. As such, it would be beneficial to perform the simulations with these faster or parallel systems, to determine if increased computing power speeds up the simulation.

Explore the use of MODFLOW interfaces other than GMS to simulate the DFN properties within the EPM model. Other MODFLOW interfaces, such as Groundwater Vistas, may allow for less computational effort for various reasons. It would be beneficial to test the model with these other interfaces to determine the least computationally intensive method for running the hybrid model.

Explore the use of groundwater transport models other than the hybrid DFN/EPM to simulate the fate and transport of contaminants in fractured aquifers. Further geotechnical investigations to refine values for parameters like fracture density, spacing, and connectivity would enable alternate models discussed in Chapter 2 to be explored. Results from these analyses could be used to validate the assumption that the

hybrid DFN/EPM is appropriate for fractured aquifers, or that another model more accurately predicts contaminant transport.

Explore optimization of pump-and-treat systems for application in fractured rock systems. This study was a preliminary look at how a pump-and-treat system might be applied in a fractured aquifer. No attempt was made to design an "optimal" system that would achieve specific performance goals at minimal cost. As such, it is recommended that the pumping layout proposed be reevaluated, to determine if the rates and locations should be adjusted to enhance removal while still providing hydraulic containment. For the purpose of simplicity in this research, which was focused on evaluating the usability of the hybrid DFN/EPM, the system was limited to the actual wells that had been installed at the site, and pumping rates were assumed constant at each well. To effectively contain a contaminant plume in fractured media utilizing a pump-and-treat system, alternative well locations, screen depths, and pumping rates should be considered to ensure plume capture.

Appendix A: Historical monitoring data from Pease AFB

Well ID	Date	TCE (µg/L)
32-4254	12/21/1994	110
32-4254	11/3/1995	360
32-4254	8/5/1996	260
32-4254	11/5/1996	200
32-4254	5/2/1997	100
32-4254	7/17/1997	73
32-4254	11/8/1997	65
32-4254	4/13/1998	35
32-4254	8/3/1998	31
32-4254	10/20/1998	530
32-4254	5/26/1999	35
32-4254	9/27/1999	826
32-4254	3/22/2000	142
32-4254	10/3/2000	99
32-4254	5/2/2001	23
32-4254	10/10/2001	17
32-4254	5/31/2002	12
32-4254	5/19/2003	5.6
32-4254	10/14/2003	4.4
32-5019	9/26/1991	36
32-5019	1/14/1992	24
32-5020	9/24/1991	0.2
32-5020	1/13/1992	1
32-5020	11/12/1996	3
32-5020	4/15/1997	1
32-5020	7/16/1997	1
32-5020	11/6/1997	17
32-5020	4/10/1998	1
32-5020	8/5/1998	0.9
32-5020	10/14/1998	1
32-5020	6/16/1999	2
32-5020	7/5/2000	0.8
32-5020	8/23/2001	1
32-5020	7/28/2003	1
32-5022	9/24/1991	0.7
32-5022	1/13/1992	0.4
32-5022	7/27/1995	0.34
32-5022	11/22/1996	120
32-5022	4/15/1997	8
32-5022	7/25/1997	8
32-5022	11/5/1997	4

Well ID	Date	TCE (µg/L)
32-5022	4/1/1998	2
32-5022	8/6/1998	1
32-5022	10/13/1998	1
32-5022	6/17/1999	2
32-5022	7/6/2000	1
32-5022	8/23/2001	1
32-5022	7/28/2003	1
32-5024	9/26/1991	190000
32-5024	1/10/1992	550000
32-5024	1/10/1992	680000
32-5024	11/11/1993	640000
32-5024	12/14/1993	930000
32-5024	3/2/1994	850000
32-5024	3/14/1994	750000
32-5024	5/17/1994	910000
32-5024	11/10/1994	820000
32-5024	5/17/1995	62000
32-5024	10/23/1995	46000
32-5024	10/27/1995	440000
32-5024	4/8/1996	31000
32-5024	7/31/1996	34000
32-5024	11/20/1996	15000
32-5024	2/20/1997	38000
32-5024	2/25/1997	220000
32-5024	2/28/1997	300000
32-5024	3/4/1997	240000
32-5024	3/11/1997	18000
32-5024	3/18/1997	150000
32-5024	4/9/1997	160000
32-5024	5/5/1997	200000
32-5024	6/11/1997	150000
32-5024	7/15/1997	290000
32-5024	8/5/1997	220000
32-5024	9/10/1997	170000
32-5024	10/14/1997	140000
32-5024	11/7/1997	150000
32-5024	11/11/1997	93000
32-5024	12/16/1997	110000
32-5024	1/19/1998	70000
32-5024	2/13/1998	66000
32-5024	3/12/1998	61000
32-5024	4/8/1998	99000
32-5024	4/15/1998	87000
32-5024	5/7/1998	69000
32-5024	6/9/1998	55000

Well ID	Date	TCE (µg/L)
32-5024	7/8/1998	64000
32-5024	8/4/1998	86000
32-5024	8/5/1998	66000
32-5024	9/1/1998	70000
32-5024	10/9/1998	62000
32-5024	10/15/1998	59000
32-5024	11/13/1998	140000
32-5024	12/8/1998	78000
32-5024	1/5/1999	140000
32-5024	2/16/1999	120000
32-5024	6/29/1999	134000
32-5024	7/19/1999	110000
32-5024	7/5/2000	78000
32-5024	8/24/2001	27000
32-5024	7/29/2003	11000
32-5025	10/1/1991	35000
32-5025	1/9/1992	460000
32-5025	11/11/1993	17000
32-5025	12/13/1993	13000
32-5025	3/2/1994	14000
32-5025	3/14/1994	14000
32-5025	5/17/1994	24000
32-5025	11/10/1994	69000
32-5025	5/17/1995	30000
32-5025	4/8/1996	94000
32-5025	8/1/1996	39000
32-5025	11/11/1996	27000
32-5031	1/15/1992	0.8
32-5031	11/13/1996	8
32-5031	4/15/1997	1
32-5031	7/30/1997	2
32-5031	11/10/1997	8
32-5031	4/2/1998	1
32-5031	8/6/1998	4
32-5031	10/19/1998	1
32-5031	6/21/1999	5
32-5031	7/5/2000	6
32-5031	8/23/2001	2.4
32-5031	7/28/2003	4.7
32-5032	1/10/1992	1
32-5032	7/20/1993	1
32-5032	11/9/1993	1
32-5032	5/17/1994	1

Well ID	Date	TCE (µg/L)
32-5032	11/10/1994	1
32-5032	5/16/1995	1
32-5032	11/1/1995	22
32-5032	4/8/1996	1
32-5032	7/31/1996	0.5
32-5032	11/19/1996	5
32-5032	4/28/1997	1
32-5032	7/23/1997	1
32-5032	11/6/1997	2
32-5032	3/31/1998	1
32-5032	7/28/1998	1
32-5032	10/20/1998	1
32-5032	6/24/1999	2
32-5032	7/10/2000	1
32-5032	8/23/2001	1
32-5032	7/29/2003	1
32-5075	10/1/1992	1
32-5075	8/5/1996	0.5
32-5075	11/13/1996	1
32-5075	4/16/1997	1
32-5075	7/15/1997	1
32-5075	11/6/1997	1
32-5075	4/15/1998	1
32-5075	8/6/1998	0.6
32-5075	10/19/1998	1
32-5076	10/1/1992	2
32-5076	6/23/1994	1
32-5076	11/10/1994	1
32-5076	5/22/1995	0.16
32-5076	11/1/1995	1
32-5076	4/8/1996	110
32-5076	7/30/1996	1
32-5076	11/14/1996	4
32-5076	4/16/1997	2
32-5076	7/15/1997	1
32-5076	11/10/1997	0.7
32-5076	4/22/1998	1
32-5076	8/10/1998	1
32-5076	10/19/1998	1
32-5076	6/22/1999	2
32-5076	7/10/2000	1
32-5076	8/23/2001	1
32-5076	7/30/2003	1

Well ID	Date	TCE (µg/L)
32-5077	9/24/1992	7
32-5087	9/25/1992	1
32-5087	4/14/1997	1
32-5087	7/14/1997	1
32-5087	11/5/1997	1
32-5087	3/25/1998	1
32-5087	8/3/1998	1
32-5087	10/19/1998	1
32-5088	9/25/1992	1
32-5088	4/7/1997	1
32-5088	7/10/1997	1
32-5088	11/5/1997	1
32-5088	3/26/1998	1
32-5088	8/4/1998	1
32-5088	10/14/1998	1
32-5142	4/13/1995	520000
32-5142	5/2/1995	430000
32-5142	5/2/1995	300000
32-5142	5/2/1995	140000
32-5142	5/2/1995	460000
32-5142	5/2/1995	370000
32-5142	5/2/1995	180000
32-5142	5/2/1995	370000
32-5142	5/2/1995	490000
32-5142	5/2/1995	440000
32-522	11/30/1988	0.6
32-522	5/6/1989	0.6
32-522	8/4/1990	0.6
32-522	9/24/1991	1
32-5266	10/6/1995	2.9
32-5266	11/2/1995	4.4
32-5266	4/9/1996	11
32-5266	7/30/1996	5
32-5266	11/14/1996	5
32-5266	4/22/1997	56
32-5266	7/24/1997	86
32-5266	11/5/1997	4
32-5266	4/21/1998	38
32-5266	8/6/1998	60
32-5266	10/19/1998	5
32-5266	6/22/1999	45
32-5266	7/10/2000	140

Well ID	Date	TCE (µg/L)
32-5266	8/23/2001	210
32-5266	7/30/2003	76
32-5267	10/23/1995	50000
32-5267	10/27/1995	35000
32-5267	11/21/1996	44000
32-5267	2/20/1997	26000
32-5267	2/25/1997	24000
32-5267	2/28/1997	40000
32-5267	3/4/1997	36000
32-5267	3/11/1997	29000
32-5267	3/18/1997	36000
32-5267	4/9/1997	37000
32-5267	5/5/1997	44000
32-5267	6/11/1997	34000
32-5267	7/15/1997	37000
32-5267	8/5/1997	54000
32-5267	9/10/1997	36000
32-5267	10/14/1997	18000
32-5267	11/6/1997	31000
32-5267	11/11/1997	22000
32-5267	12/16/1997	23000
32-5267	1/19/1998	20000
32-5267	2/13/1998	26000
32-5267	3/12/1998	27000
32-5267	4/8/1998	28000
32-5267	4/15/1998	49000
32-5267	5/7/1998	39000
32-5267	6/9/1998	24000
32-5267	7/8/1998	30000
32-5267	8/4/1998	23000
32-5267	8/5/1998	16000
32-5267	9/1/1998	13000
32-5267	10/9/1998	11000
32-5267	10/15/1998	19000
32-5267	11/13/1998	23000
32-5267	12/8/1998	18000
32-5267	1/5/1999	21000
32-5267	2/16/1999	30000
32-5267	6/29/1999	25900
32-5267	7/19/1999	30000
32-5267	7/5/2000	39000
32-5267	8/24/2001	12000
32-5267	7/29/2003	9400
32-5268	10/23/1995	230000

Well ID	Date	TCE (µg/L)
32-5268	10/27/1995	170000
32-5268	11/20/1996	180000
32-5268	2/20/1997	210000
32-5268	2/25/1997	240000
32-5268	2/28/1997	350000
32-5268	3/4/1997	280000
32-5268	3/11/1997	170000
32-5268	3/18/1997	210000
32-5268	4/9/1997	180000
32-5268	5/5/1997	150000
32-5268	6/11/1997	160000
32-5268	7/15/1997	130000
32-5268	8/5/1997	52000
32-5268	9/10/1997	42000
32-5268	10/14/1997	39000
32-5268	11/6/1997	40000
32-5268	11/11/1997	58000
32-5268	12/16/1997	58000
32-5268	1/19/1998	67000
32-5268	2/13/1998	49000
32-5268	3/12/1998	52000
32-5268	4/8/1998	67000
32-5268	4/15/1998	75000
32-5268	5/7/1998	27000
32-5268	7/8/1998	45000
32-5268	8/4/1998	56000
32-5268	8/5/1998	56000
32-5268	9/1/1998	53000
32-5268	10/9/1998	46000
32-5268	10/15/1998	44000
32-5268	11/13/1998	48000
32-5268	12/8/1998	30000
32-5268	1/5/1999	45000
32-5268	2/16/1999	25000
32-5268	6/29/1999	89800
32-5268	7/19/1999	18000
32-5268	7/5/2000	9800
32-5268	8/24/2001	1400
32-5268	7/29/2003	6200
32-548	12/9/1988	10000
32-548	8/3/1990	4000
32-569	8/3/1990	0.6
32-569	9/27/1991	5
32-569	1/13/1992	1

Well ID	Date	TCE (µg/L)
32-570	8/3/1990	140
32-570	9/25/1991	120
32-570	1/15/1992	260
32-570	11/19/1993	43
32-570	5/16/1994	36
32-570	11/10/1994	3.8
32-570	5/22/1995	3.3
32-570	11/1/1995	54
32-570	4/5/1996	25
32-570	7/31/1996	26
32-570	11/11/1996	20
32-570	4/24/1997	4
32-570	7/25/1997	0.7
32-570	11/6/1997	1
32-570	4/14/1998	0.6
32-570	8/4/1998	1
32-570	10/14/1998	0.5
32-570	6/30/1999	2
32-570	7/11/2000	1
32-570	8/23/2001	15
32-570	7/29/2003	0.77
32-571	8/3/1990	0.6
32-571	9/24/1991	2
32-571	1/15/1992	35
32-571	11/12/1996	4
32-571	4/18/1997	1
32-571	7/24/1997	1
32-571	11/6/1997	0.6
32-571	4/21/1998	0.8
32-571	8/4/1998	1
32-571	10/14/1998	1
32-571	6/15/1999	2
32-571	7/5/2000	4
32-571	8/23/2001	1
32-571	7/29/2003	1
32-573	8/3/1990	27
32-573	9/24/1991	140
32-573	1/15/1992	200
32-573	11/19/1993	42
32-573	5/18/1994	10
32-573	11/9/1994	6.3
32-573	5/22/1995	2.6
32-573	11/3/1995	9
32-573	4/8/1996	22

Well ID	Date	TCE (µg/L)
32-573	7/31/1996	14
32-573	11/15/1996	80
32-573	4/4/1997	32
32-573	4/7/1997	38
32-573	7/24/1997	8
32-573	11/5/1997	1
32-573	4/1/1998	1
32-573	8/5/1998	2
32-573	10/13/1998	0.6
32-573	6/23/1999	2
32-573	7/6/2000	0.7
32-573	8/22/2001	0.53
32-573	7/28/2003	1
32-574	8/3/1990	0.6
32-574	9/24/1991	0.5
32-574	1/13/1992	1
32-574	11/9/1993	1
32-574	5/17/1994	1
32-574	11/11/1994	1
32-574	5/25/1995	1
32-574	4/9/1996	7
32-574	8/1/1996	37
32-574	11/19/1996	12
32-574	4/28/1997	1
32-574	7/23/1997	1
32-574	11/7/1997	1
32-574	3/27/1998	1
32-574	7/27/1998	1
32-574	10/20/1998	0.7
32-574	6/24/1999	2
32-574	7/6/2000	1
32-574	8/23/2001	1
32-574	7/31/2003	1
32-6008	9/24/1991	89
32-6008	1/15/1992	61
32-6008	6/29/1993	120
32-6008	8/4/1993	51
32-6008	8/24/1993	48
32-6008	9/23/1993	56
32-6008	11/9/1993	56
32-6008	5/18/1994	50
32-6008	11/9/1994	11
32-6008	5/22/1995	2.4
32-6008	11/3/1995	21

Well ID	Date	TCE (µg/L)
32-6008	4/8/1996	76
32-6008	7/31/1996	58
32-6008	11/15/1996	340
32-6008	4/10/1997	52
32-6008	4/10/1997	73
32-6008	4/10/1997	50
32-6008	7/29/1997	14
32-6008	11/5/1997	6
32-6008	4/1/1998	0.7
32-6008	8/10/1998	0.8
32-6008	10/13/1998	0.7
32-6008	6/23/1999	2
32-6008	7/6/2000	0.7
32-6008	8/23/2001	1
32-6008	7/31/2003	1
32-6012	9/25/1991	270
32-6012	1/10/1992	170
32-6012	8/3/1993	55
32-6012	11/11/1993	62
32-6012	5/18/1994	31
32-6012	11/10/1994	7
32-6012	5/25/1995	7
32-6012	4/9/1996	14
32-6012	8/1/1996	5
32-6012	11/11/1996	19
32-6012	4/8/1997	14
32-6012	7/10/1997	22
32-6012	11/7/1997	11
32-6012	3/30/1998	5
32-6012	7/27/1998	2
32-6012	10/8/1998	2
32-6012	6/21/1999	2
32-6012	7/10/2000	2
32-6012	8/27/2001	0.77
32-6012	7/31/2003	1
32-6014	10/1/1991	--
32-6014	1/10/1992	15000
32-6014	1/10/1992	--
32-6014	11/18/1993	45000
32-6014	5/17/1994	110000
32-6014	11/9/1994	73000
32-6027	1/15/1992	0.5
32-6027	8/3/1993	1

Well ID	Date	TCE (µg/L)
32-6027	9/23/1993	1
32-6027	11/11/1993	1
32-6027	5/17/1994	0.3
32-6027	11/10/1994	1
32-6027	4/9/1996	5
32-6027	7/31/1996	0.5
32-6027	11/13/1996	1
32-6027	4/15/1997	1
32-6027	7/30/1997	1
32-6027	11/10/1997	1
32-6027	4/14/1998	1
32-6027	8/11/1998	1
32-6027	10/20/1998	1
32-6027	6/21/1999	2
32-6027	7/10/2000	1
32-6027	8/23/2001	1
32-6027	7/30/2003	1
32-6029	1/15/1992	550
32-6029	11/18/1993	590
32-6029	5/17/1994	450
32-6029	11/9/1994	250
32-6029	5/30/1995	140
32-6029	11/2/1995	73
32-6029	4/15/1996	250
32-6029	8/5/1996	170
32-6029	11/15/1996	220
32-6029	4/22/1997	57
32-6029	7/15/1997	670
32-6029	11/6/1997	570
32-6029	4/14/1998	920
32-6029	8/11/1998	3200
32-6029	10/13/1998	1
32-6029	5/26/1999	470
32-6029	9/21/1999	19
32-6029	3/14/2000	333
32-6029	10/3/2000	1480
32-6029	5/1/2001	140
32-6029	10/10/2001	980
32-6029	5/30/2002	92
32-6029	5/5/2003	120
32-6029	10/16/2003	170
32-6031	1/10/1992	1
32-6031	7/20/1993	0.4
32-6031	11/9/1993	1

Well ID	Date	TCE (µg/L)
32-6031	5/17/1994	2
32-6031	11/11/1994	3
32-6031	5/16/1995	1.1
32-6031	4/8/1996	2
32-6031	7/31/1996	2
32-6031	11/19/1996	1
32-6031	4/3/1997	1
32-6031	4/3/1997	1
32-6031	7/21/1997	0.9
32-6031	11/6/1997	7
32-6031	3/31/1998	0.7
32-6031	7/28/1998	0.6
32-6031	10/13/1998	0.6
32-6031	6/24/1999	2
32-6031	7/10/2000	1
32-6031	8/27/2001	1
32-6031	7/29/2003	1
32-6033	1/10/1992	93000
32-6033	3/16/1992	3
32-6033	3/31/1993	4
32-6033	7/20/1993	9
32-6033	11/9/1993	9
32-6033	5/17/1994	8
32-6033	11/11/1994	6.6
32-6033	5/16/1995	5.6
32-6033	4/8/1996	6
32-6033	7/31/1996	7
32-6033	11/19/1996	7
32-6033	4/25/1997	7
32-6033	7/22/1997	5
32-6033	11/6/1997	8
32-6033	3/31/1998	5
32-6033	7/28/1998	4
32-6033	10/13/1998	4
32-6033	6/24/1999	3
32-6033	7/6/2000	2
32-6033	8/23/2001	0.76
32-6033	7/29/2003	1
32-6042	1/15/1992	410
32-6042	10/13/1992	153
32-6042	11/18/1993	330
32-6042	5/17/1994	150
32-6042	11/9/1994	170
32-6042	5/24/1995	320

Well ID	Date	TCE (µg/L)
32-6042	11/2/1995	110
32-6042	4/9/1996	120
32-6042	7/30/1996	60
32-6042	11/12/1996	290
32-6042	4/17/1997	3
32-6042	7/16/1997	0.9
32-6042	11/7/1997	12
32-6042	4/23/1998	0.8
32-6042	8/4/1998	0.5
32-6042	10/15/1998	1
32-6042	6/15/1999	2
32-6042	7/5/2000	1
32-6042	8/27/2001	0.81
32-6042	8/1/2003	1.4
32-6060	9/30/1992	220
32-6060	6/29/1993	200
32-6060	8/4/1993	130
32-6060	8/24/1993	130
32-6060	9/23/1993	97
32-6060	11/9/1993	110
32-6060	5/16/1994	62
32-6060	11/10/1994	19
32-6060	5/22/1995	17
32-6060	4/5/1996	74
32-6060	7/31/1996	98
32-6060	11/6/1996	2
32-6061	9/25/1992	1
32-6061	4/8/1997	1
32-6061	7/10/1997	19
32-6061	11/8/1997	1
32-6061	3/26/1998	1
32-6061	8/4/1998	1
32-6061	10/14/1998	1
32-6061	6/16/1999	2
32-6061	7/11/2000	1
32-6061	8/28/2001	1
32-6061	7/31/2003	1
32-6062	9/25/1992	1
32-6063	10/2/1992	3
32-6063	11/12/1993	2
32-6063	5/18/1994	2
32-6063	11/10/1994	2

Well ID	Date	TCE (µg/L)
32-6063	5/24/1995	1.4
32-6063	4/9/1996	2
32-6063	7/30/1996	2
32-6063	11/21/1996	2
32-6063	4/28/1997	2
32-6063	7/21/1997	2
32-6063	11/6/1997	2
32-6063	3/26/1998	0.9
32-6063	7/23/1998	2
32-6063	10/14/1998	2
32-6063	6/28/1999	2
32-6063	7/6/2000	2
32-6063	8/28/2001	1.2
32-6064	9/24/1992	1
32-6064	6/29/1993	1
32-6064	8/4/1993	1
32-6064	8/25/1993	1
32-6064	9/23/1993	1
32-6064	11/12/1996	4
32-6064	4/15/1997	0.8
32-6064	7/16/1997	2
32-6064	11/6/1997	5
32-6064	4/10/1998	0.5
32-6064	8/10/1998	0.5
32-6064	10/19/1998	1
32-6064	6/16/1999	2
32-6064	7/5/2000	1
32-6064	8/28/2001	1
32-6064	7/31/2003	1
32-6066	9/29/1992	1
32-6066	8/3/1993	110
32-6069	10/1/1992	1
32-6069	4/8/1997	1
32-6069	7/28/1997	1
32-6069	11/10/1997	1
32-6069	3/30/1998	1
32-6069	8/4/1998	1
32-6069	10/14/1998	1
32-6070	9/25/1992	1
32-6070	4/14/1997	1
32-6070	7/15/1997	1
32-6070	11/6/1997	1

Well ID	Date	TCE (µg/L)
32-6070	4/13/1998	1
32-6070	8/5/1998	1
32-6070	10/15/1998	1
32-6070	6/17/1999	2
32-6070	6/29/2000	1
32-6070	8/28/2001	1
32-6070	8/5/2003	1
32-6071	9/30/1992	1
32-6071	8/3/1993	1
32-6071	11/13/1996	1
32-6071	4/17/1997	1
32-6071	7/25/1997	1
32-6071	11/7/1997	1
32-6071	4/10/1998	1
32-6071	8/11/1998	1
32-6071	10/15/1998	1
32-6072	10/2/1992	0.6
32-6072	11/12/1993	1
32-6072	5/18/1994	1
32-6072	11/10/1994	1
32-6072	5/24/1995	1.6
32-6072	4/9/1996	6
32-6072	7/31/1996	2
32-6072	11/21/1996	3
32-6072	4/28/1997	2
32-6072	7/18/1997	2
32-6072	11/6/1997	7
32-6072	3/26/1998	2
32-6072	7/23/1998	2
32-6072	10/14/1998	2
32-6072	6/28/1999	2
32-6072	7/6/2000	1
32-6072	8/28/2001	0.9
32-6072	8/1/2003	1
32-6073	9/9/1992	12282
32-6073	9/14/1992	9524
32-6073	10/1/1992	16000
32-6073	9/23/1993	9400
32-6073	11/18/1993	2800
32-6073	5/17/1994	840
32-6073	11/9/1994	8000
32-6073	5/24/1995	8100
32-6073	10/23/1995	34000

Well ID	Date	TCE (µg/L)
32-6073	10/27/1995	7000
32-6073	11/6/1995	6800
32-6073	4/15/1996	4300
32-6073	8/5/1996	4500
32-6073	11/21/1996	360
32-6073	2/20/1997	2800
32-6073	2/25/1997	2500
32-6073	2/28/1997	2100
32-6073	3/4/1997	2300
32-6073	3/11/1997	1700
32-6073	3/18/1997	1300
32-6073	4/9/1997	680
32-6073	5/5/1997	390
32-6073	6/11/1997	33
32-6073	7/15/1997	240
32-6073	8/5/1997	250
32-6073	9/10/1997	300
32-6073	10/14/1997	190
32-6073	11/8/1997	290
32-6073	11/11/1997	270
32-6073	12/16/1997	460
32-6073	1/19/1998	450
32-6073	2/13/1998	360
32-6073	3/12/1998	370
32-6073	4/8/1998	560
32-6073	4/15/1998	700
32-6073	5/7/1998	680
32-6073	6/9/1998	280
32-6073	7/8/1998	230
32-6073	8/4/1998	300
32-6073	8/5/1998	310
32-6073	9/1/1998	180
32-6073	10/9/1998	190
32-6073	10/15/1998	170
32-6073	11/13/1998	270
32-6073	12/8/1998	190
32-6073	1/5/1999	290
32-6073	2/16/1999	280
32-6073	6/23/1999	242
32-6073	7/19/1999	430
32-6073	7/5/2000	280
32-6073	8/24/2001	69
32-6073	8/1/2003	39
32-6074	9/9/1992	777332
32-6074	9/16/1992	728019

Well ID	Date	TCE (µg/L)
32-6074	10/2/1992	390000
32-6074	6/29/1993	490000
32-6074	8/4/1993	560000
32-6074	8/24/1993	730000
32-6074	9/23/1993	710000
32-6074	11/11/1993	450000
32-6074	12/13/1993	760000
32-6074	3/2/1994	270000
32-6074	3/14/1994	590000
32-6074	5/17/1994	790000
32-6074	11/10/1994	940000
32-6074	5/17/1995	440000
32-6074	10/23/1995	600000
32-6074	10/27/1995	620000
32-6074	4/8/1996	530000
32-6074	7/31/1996	840000
32-6074	11/20/1996	770000
32-6074	2/20/1997	520000
32-6074	2/25/1997	420000
32-6074	2/28/1997	310000
32-6074	3/4/1997	410000
32-6074	3/11/1997	290000
32-6074	3/18/1997	210000
32-6074	4/9/1997	190000
32-6074	5/5/1997	160000
32-6074	6/11/1997	150000
32-6074	7/15/1997	120000
32-6074	8/5/1997	240000
32-6074	9/10/1997	110000
32-6074	10/14/1997	120000
32-6074	11/8/1997	96000
32-6074	11/11/1997	72000
32-6074	12/16/1997	51000
32-6074	1/19/1998	51000
32-6074	2/13/1998	50000
32-6074	3/12/1998	54000
32-6074	4/8/1998	72000
32-6074	4/15/1998	86000
32-6074	5/7/1998	92000
32-6074	6/9/1998	84000
32-6074	7/8/1998	67000
32-6074	8/4/1998	69000
32-6074	8/5/1998	71000
32-6074	9/1/1998	59000
32-6074	10/9/1998	88000
32-6074	10/20/1998	52000

Well ID	Date	TCE (µg/L)
32-6074	11/13/1998	84000
32-6074	12/8/1998	58000
32-6074	1/5/1999	85000
32-6074	2/16/1999	75000
32-6074	6/29/1999	46700
32-6074	7/19/1999	50000
32-6074	7/5/2000	45000
32-6074	8/24/2001	6300
32-6074	8/1/2003	2000
32-6122	9/17/1993	61000
32-6122	9/20/1993	920
32-6122	12/3/1993	420000
32-6127	12/19/1994	310
32-6127	12/19/1994	180
32-6127	5/25/1995	130
32-6127	11/2/1995	180
32-6127	11/22/1996	80
32-6127	4/21/1997	48
32-6127	7/29/1997	36
32-6127	11/11/1997	17
32-6127	4/23/1998	17
32-6127	8/11/1998	18
32-6127	10/19/1998	22
32-6127	6/28/1999	2
32-6127	7/11/2000	3
32-6127	8/28/2001	1.6
32-6127	8/1/2003	12
32-6132	11/2/1995	400
32-6132	4/9/1996	93
32-6132	7/31/1996	140
32-6132	11/14/1996	85
32-6132	4/21/1997	102
32-6132	7/29/1997	110
32-6132	11/7/1997	170
32-6132	4/21/1998	180
32-6132	8/6/1998	130
32-6132	10/19/1998	110
32-6132	6/22/1999	115
32-6132	7/10/2000	81
32-6132	8/27/2001	44
32-6132	7/30/2003	40
32-6134	10/23/1995	63000

Well ID	Date	TCE (µg/L)
32-6134	10/27/1995	44000
32-6134	4/16/1996	110000
32-6134	8/2/1996	100000
32-6134	11/22/1996	86000
32-6134	2/20/1997	66000
32-6134	2/25/1997	91000
32-6134	2/28/1997	120000
32-6134	3/4/1997	99000
32-6134	3/11/1997	79000
32-6134	3/18/1997	75000
32-6134	4/9/1997	59000
32-6134	5/5/1997	59000
32-6134	6/11/1997	63000
32-6134	7/15/1997	44000
32-6134	8/5/1997	1700
32-6134	9/10/1997	11000
32-6134	10/14/1997	4800
32-6134	11/8/1997	13000
32-6134	11/11/1997	11000
32-6134	12/16/1997	28000
32-6134	1/19/1998	22000
32-6134	2/13/1998	22000
32-6134	3/12/1998	22000
32-6134	4/8/1998	14000
32-6134	4/15/1998	25000
32-6134	5/7/1998	2200
32-6134	6/9/1998	24000
32-6134	7/8/1998	13000
32-6134	8/4/1998	14000
32-6134	8/5/1998	12000
32-6134	9/1/1998	12000
32-6134	10/9/1998	10000
32-6134	10/20/1998	9100
32-6134	11/13/1998	8400
32-6134	12/8/1998	6600
32-6134	1/5/1999	3500
32-6134	2/16/1999	3800
32-6134	6/29/1999	884
32-6134	7/19/1999	2200
32-6134	7/5/2000	1900
32-6134	8/24/2001	670
32-6134	8/1/2003	1500
32-6135	11/14/1995	2900
32-6135	4/11/1996	3100
32-6135	7/31/1996	4500

Well ID	Date	TCE (µg/L)
32-6135	11/11/1996	3100
32-6135	4/18/1997	1500
32-6135	7/24/1997	900
32-6135	11/7/1997	910
32-6135	4/24/1998	730
32-6135	8/6/1998	300
32-6135	10/21/1998	290
32-6135	6/15/1999	138
32-6135	7/6/2000	61
32-6135	8/27/2001	15
32-6135	7/31/2003	7.4
32-6141	10/23/1995	8100
32-6141	10/27/1995	6800
32-6141	11/2/1995	12000
32-6141	4/16/1996	4800
32-6141	8/5/1996	4000
32-6141	11/20/1996	7700
32-6141	2/20/1997	5200
32-6141	2/25/1997	3900
32-6141	2/28/1997	5100
32-6141	3/4/1997	3600
32-6141	3/11/1997	3000
32-6141	3/18/1997	2900
32-6141	4/9/1997	2400
32-6141	5/5/1997	1800
32-6141	6/11/1997	1400
32-6141	7/15/1997	1300
32-6141	8/5/1997	1500
32-6141	9/10/1997	1200
32-6141	10/14/1997	1300
32-6141	11/10/1997	1300
32-6141	11/11/1997	1400
32-6141	12/16/1997	660
32-6141	1/19/1998	560
32-6141	2/13/1998	470
32-6141	3/12/1998	570
32-6141	4/8/1998	510
32-6141	4/15/1998	610
32-6141	5/7/1998	560
32-6141	6/9/1998	470
32-6141	7/8/1998	440
32-6141	8/4/1998	550
32-6141	8/5/1998	470
32-6141	9/1/1998	440
32-6141	10/9/1998	380

Well ID	Date	TCE (µg/L)
32-6141	10/20/1998	350
32-6141	11/13/1998	140
32-6141	12/8/1998	320
32-6141	1/5/1999	430
32-6141	2/16/1999	360
32-6141	6/29/1999	355
32-6141	7/19/1999	320
32-6141	7/5/2000	210
32-6141	8/24/2001	94
32-6141	7/31/2003	18
32-616	12/13/1988	2.8
32-616	5/16/1989	2.4
32-616	5/16/1989	5.1
32-616	8/3/1990	2.9
32-616	9/27/1991	980
32-616	1/15/1992	480
32-616	6/29/1993	380
32-616	8/5/1993	22000
32-616	8/25/1993	22000
32-616	9/21/1993	23000
32-616	9/21/1993	24000
32-616	11/1/1993	8100
32-616	11/18/1993	10000
32-616	12/14/1993	6500
32-616	3/2/1994	4500
32-616	3/14/1994	4800
32-616	5/17/1994	3900
32-616	10/17/1994	1600
32-616	5/16/1995	1400
32-616	11/6/1995	490
32-616	4/8/1996	4300
32-616	7/30/1996	720
32-616	11/22/1996	1100
32-616	11/7/1997	61
32-616	4/23/1998	120
32-616	8/12/1998	55
32-616	10/21/1998	46
32-632	8/3/1990	2.5
32-632	9/24/1991	5
32-632	1/15/1992	40
32-632	11/9/1993	11
32-632	5/18/1994	34
32-632	11/11/1994	14
32-632	5/22/1995	4.9

Well ID	Date	TCE (µg/L)
32-632	11/3/1995	13
32-632	4/8/1996	23
32-632	7/30/1996	29
32-632	11/25/1996	94
32-632	4/4/1997	35
32-632	4/7/1997	67
32-632	7/30/1997	32
32-632	11/5/1997	20
32-632	4/1/1998	21
32-632	8/5/1998	15
32-632	10/13/1998	12
32-632	6/23/1999	8
32-632	7/17/2000	4
32-632	8/28/2001	1.3
32-632	7/31/2003	1
32-633	8/3/1990	0.6
32-633	9/24/1991	0.5
32-633	1/13/1992	3
32-633	11/19/1996	4
32-633	4/29/1997	3
32-633	7/23/1997	3
32-633	11/7/1997	5
32-633	3/30/1998	3
32-633	7/27/1998	3
32-633	10/15/1998	3
32-7205	11/10/1997	1
32-7205	4/15/1998	1
32-7205	8/3/1998	1
32-7205	10/21/1998	1
32-7548	11/13/1992	5
32-7854	11/14/1996	110
32-7854	4/18/1997	67
32-7854	7/16/1997	13
32-7854	11/10/1997	4
32-7854	4/23/1998	1
32-7854	8/12/1998	0.7
32-7854	10/21/1998	2
32-7854	6/15/1999	2
32-7854	7/6/2000	0.6
32-7854	8/27/2001	0.69
32-7854	7/30/2003	0.53

Bibliography

Air Force Base Closure Agency (AFBCA). "Pease AFB site 32/36 source area modeling," http://www.adminrec.com/documents2/ADMINREC/PEASE/CD9/DATA/9/70/MULTI.PDF. September 1994.

Air Force Base Closure Agency (AFBCA). "Pease AFB site 32 source control options letter report," http://www.adminrec.com/documents2/ADMINREC/PEASE/CD9/DATA/3/72/MULTI.PDF. February 1995.

Anderson, Mary P. and William W. Woessner. *Applied Groundwater Modeling: Simulation of Flow and Advective Transport*. San Diego, CA: Academic Press, Inc., 1992.

Baecher, G. B., N. A. Lanney and H. H. Einstein. "Statistical Description of Rock Properties and Sampling," Proceedings of the 18th U.S. Symposium on Rock Mechanics, American Institute of Mining Engineers, 5C1-8 (1977).

Bakker, M and O.D.L. Strack. "Capture zone delineation in two-dimensional groundwater flow models," Water Resources Research 32: 1309-1315 (May 1996).

Basha, H.A. and W. El-Asmar. "The fracture flow equation and its perturbation solution," *Water Resources Research*, 39(12): 191-206 (December 2003).

Bear, J., C.F. Tsang, and G. de Marsily. *Flow and Contaminant Transport in Fractured Rock*. San Diego, CA: Academic Press, Inc., 1993.

Becker, M.W. and A.M. Shapiro. "Tracer transport in fractured crystalline rock: evidence of nondiffusive breakthrough tailing," *Water Resources Research*, 36(7): 1677-1686 (2000).

Bedient, Philip B., Hanadi S. Rifai, and Charles J. Newell. *Ground Water Contamination: Transport and Remediation.* Upper Saddle River, NJ: Prentice-Hall, Inc., 1999.

Berkowitz, Brian. "Characterizing flow and transport in fractured geological media: A review," *Advances in Water Resources*, 25: 861-884 (11 March 2002).

Berkowitz, B. and H. Scher. "Anomalous transport in random fracture networks," *Physics Review Letters*, 79: 4038-4041 (1997).

Berkowitz, B. and H. Scher. "Theory of anomalous chemical transport in fracture networks," *Physics Review E*, 57: 5858-5869 (1998).

Cacas, M. C., E. Ledoux, G. de Marsily, and B. Tillie. "Modeling fracture flow with a stochastic discrete fracture network: Calibration and validation 1. The flow model," *Water Resources Research*, 26: 479-489 (March 1990a).

Cacas, M. C. E. Ledoux, and G. de Marsily. "Modeling fracture flow with a stochastic discrete fracture network: Calibration and validation 1. The transport model," *Water Resources Research*, 26: 491-500 (March 1990b)

Charbeneau, R.J. Groundwater hydraulics and pollutant transport. Upper Saddle River: Prentice-Hall, Inc., 2000.

Clark, Alexandra. Hydrogeologist, Golder Associates, Portland OR. Personal Correspondence. October 2004.

de Josselin de Jong, G. and C.A. Way. "Dispersion in fissured rock," report, 30pp, New Mexico Institute of Mining and Technology, Socorro (1972).

Department of the Interior. "Hydrology of Fractured Rocks." http://water.usgs.gov/nrp/proj.bib/ hsieh.html. 14 April 2004.

Dershowitz, W. S. "Rock Joint Systems" Ph.D. Dissertation, Massachusetts Institute of Technology, Cambridge, MA (1984).

Dershowitz, William S., Paul R. La Pointe, and Thomas W. Doe. "Advances in Discrete Fracture Network Modeling." *Proceedings of the 2004 USEPA/NGWA Fractured Rock Conference*. September 2004.

Domenico, Patrick A. and Franklin W. Schwartz. *Physical and Chemical Hydrogeology*. New York: John Wiley and Sons, Inc., 1998.

Durham, W.B. and B.P. Bonner. "Self-propping and fluid flow in slightly offset joints at high effective pressures," *Journal of Geophysical Research*, 99(B5): 9391-9 (1994).

Einarson, Murray D. and Douglas M. Mackay. "Predicting Impacts of Groundwater Contamination," *Environmental Science and Technology*, 35: 66-73 (1 February 2001).

Freeze, R. Allan and John A. Cherry. *Groundwater*. Englewood Cliffs, N.J: Prentice-Hall, Inc., 1979.

Gale, J.E. "Assessing the permeability characteristics of fractured rock," *Geological Society of America Special Paper 189*: 163-181 (1982).

Gale, J.E. and K.G. Raven. Effect of sample size on stress permeability relationship for natural fractures, Technical Information Report No. 48, LBL-11865, SAC-48, UC-70 (1980).

Gale, J.E., A. Rouleau, and L.C. Atkison. "Hydraulic properties of fractures," Proceedings of the 17th International Congress of International Association of Hydrogeologists, Tucson, AZ, 17: 1-16, (1985).

Gelhar, L.W., C. Welty, and K.R. Rehfeldt. "A critical review of data on field-scale dispersion in aquifers," *Water Resources Research*, 28: 1955-1974 (1992).

Hadermann, J. and W. Heer. "The Grimsel (Switzerland) migration experiment: integrating field experiments, laboratory investigations and modeling," *Journal of Contaminant Hydrology*, 21(1-4): 87-100 (1996).

Hamm, S.Y. and P. Bidaux. "Dual-porosity fractal models for transient flow analysis in fissured rocks," *Water Resources Research*, 32: 2733-2745 (September 1996).

Hartman, Dean H. Expeditious Methods for Site Characterization and Risk Assessment at Department of Defense Hazardous Waste Sites in the Republic of Korea. MS Thesis, AFIT/ENV/99M-07. School of Engineering, Air Force Institute of Technology (AU), Wright-Patterson AFB, OH, March 1999.

Hassan, Ahmed E. "Validation of Numerical Ground Water Models Used to Guide Decision Making," Ground Water, 42: 277-290 (2004a).

Hassan, A.E. "A methodology for validating numerical ground water models," *Ground Water*, 42(3): 347-362 (2004b).

Huang, W., G.D. Donato, and M.J. Blunt. "Comparison of streamline-based and grid-based dual porosity simulation," *Journal of Petroleum Science and Engineering*, 43: 129-137 (2004).

Keller, A.A., P.V. Roberts, and P.K. Kitanidis. "Prediction of single-phase transport parameters in a variable aperture fracture," *Geophysical Research Letters*, (22(11): 1425-8 (1995).

Kim, J., F.W. Schwartz, L. Smith, and M. Ibaraki. "Complex dispersion in simple fractured media," *Water Resources Research*, 40: 1029-1039 (2004).

Konikow, Leonard F. "The value of postaudits in Groundwater Model Applications," in *Groundwater Models for Resources Analysis and Management.* Ed. Aly I. El-Kadi. Boca Raton, FL: CRC Press, Inc., 1995.

Lee, C.H. and I. Farmer. *Fluid Flow in Discontinuous Rocks*. London: Chapman and Hall, 1993.

Lee, J.Y. and K.K. Lee. "Analysis of the quality of parameter estimates from repeated pumping and slug tests in a fractured porous aquifer system in Wonju, Korea," *Ground Water*, 37: 692-699 (May 1999).

Lee, S.H., M.F. Lough, and C.L. Jensen. "Hierarchical modeling of flow in naturally fractured formations with multiple length scales," *Water Resources Research*, 37: 443-455 (March, 2001).

Lomize, G.M. *Seepage in Fissured Rocks*. Moscow-Leningrad: State Press, 1951.

Long, J.C.S., and D.M. Billaux. "From field data to fracture network modeling," *Water Resources Research*, 23: 1201-1216 (1987).

McCarty, Perry L., Mark N. Goltz, Gary D. Hopkins, Mark E. Dolan, Jason P. Allan, Brett T. Kawakami, and T.S. Carrothers. "Full scale evaluation of in-situ cometabolic degradation of trichloroethylene in groundwater through toluene injection," *Environmental Science and Technology*, 32: 88-100 (January 1998).

Moore, R.B. "Geohydrology and water quality of stratified-drift aquifers in the Exeter, Lamprey, and Oyster River Basins, Southeastern, New Hampshire," US Geological Survey Water-Resources Investigations Report: 88-4128 (1990).

MWH Americas, Inc. Zone 3 2003 Annual Report, former Pease AFB, Portsmouth, New Hampshire (April 2004).

National Research Council (NRC). *Ground Water Models*. Washington, D.C.: National Academy Press, 1990.

National Research Council (NRC). *Conceptual Models of Flow and Transport in the Fractured Vadose Zone.* Washington D.C.: National Academy Press, 2001.

Novakowski, K.S., P.A. Lapcevic, J. Voralek, and G. Bickerton. "Preliminary interpretation of tracer experiments conducted in a discrete rock fracture under conditions of natural flow," *Geophysical Research Letters*, 22(11): 1417-20 (1995).

Oda, M. "Permeability tensor for discontinuous rock masses," *Geotechnique*, 35: 483-495 (1985).

Osan Air Base Civil Engineering (Osan AB CE). Well bore data and contaminant concentrations provided for several drinking water wells on Osan AB. Provided by Dr. Mark N. Goltz (Professor of Engineering and Environmental Management, Air Force Institute of Technology (AFIT), Wright Patterson Air Force Base (WPAFB), Ohio) during Window on Asia Proposal: Applicability of horizontal flow treatment wells to manage groundwater contamination at US installations in Korea.

Pankow, J.F., R.L. Johnson, J.P. Hewetson, and J.A. Cherry. "An evaluation of contaminant migration patterns at two waste disposal sites on fractured porous media in terms of the equivalent porous medium (EPM) model," *Journal of Contaminant Hydrology*, 1: 65-76 (1986).

Park, Y.J., K.K. Lee, G. Kosakowski, and B. Berkowitz. "Transport behavior in three-dimensional fracture intersections," *Water Resources Research*, 39: 1215-1224 (2003).

Popper, K. *The Logic of Scientific Discovery*. New York: Routledge, 2002.

Preuss, K., and T.N. Narasimhan. "A practical method for modeling fluid and heat flow in fractured porous media," *Society of Petroleum Engineer Journal*, 25: 14-26 (1985).

Rasmuson, A. and I. Neretnieks. "Radionuclide transport in fast channels in crystalline rock," *Water Resources Research*, 22: 1247-56 (1986).

Schwartz, F.W. and H. Zhang. *Fundamentals of Ground Water*. New York: John Wiley and Sons, Inc., 2003.

Selroos, Jan-Olof, Douglas D. Walker, Anders Strom, Bjorn Gylling, and Sven Follin. "Comparison of alternative modeling approaches for groundwater flow in fractured rock," *Journal of Hydrology*, 257: 174-188 (1 February 2002).

Serco Assocurrance. ConnectFlow Software, user documentation. Harwell, UK, 2004.

Smellie, J.A.T., and M. Laaksoharju. "The Aspo hard rock laboratory: final evaluation of the hydrogeochemical pre-investigations in relation to existing geologic and hydraulic conditions," Stockholm SKB (Swedish Nuclear Fuel Waste Handling Company), Publication No. TR 92-31 (1992).

Smith, L., and F.W. Schwartz. "An analysis of the influence of fracture geometry on mass transport in fractured media," *Water Resources Research*, 20: 1241-1252 (1984).

Snow, D. A parallel plate model of fractured permeable media. PhD Dissertation, University of California, Berkeley, CA, 1965.

Solley, W. B., R. R. Pierce, and H. A. Perlman. "Estimated Use of Water in the United States in 1990," 76. U.S. Geol. Survey Circular 1081, 1993.

Staples, Michael R. An Analysis of Horizontal Flow Treatment Well Applicability for the Treatment of Chlorinated Solvent Contaminated Groundwater at United States Forces Korea Installations. MS Thesis, AFIT/GEE/ENV/02M-14. School of Engineering and Environmental Management, AFIT, Air University, WPAFB, OHIO, March 2002.

Stekl, P.J. and S.M. Flanagan. "Geohydrology and water quality of stratified-drift aquifers in the Lower Merrimack and Coastal River Basins, Southeastern, New Hampshire," US Geological Survey Water-Resources Investigations Report: 91-4025 (1992).

Strategic Environmental Research and Development Program (SERDP) and DOD Environmental Security Technology Certification Program (ESTCP). "Final Report: SERDP/ESTCP Expert Panel Workshop on Research and Development Needs for Cleanup of Chlorinated Solvent Sites." Washington, D.C., 2002.

Teideman, C.R., D.J. Goode, and P.A. Hseih. "Numerical simulation of ground water flow through glacial deposits and crystalline bedrock in the Mirror Lake Area, Grafton County, New Hampshire," US Geological Survey Professional Paper: 1572-1612 (1997).

Thiel, K. *Rock mechanics in hydroengineering*. Amsterdam-New York: Elsevier, 1989.

Tsang, Y.W. "The effect of tortuosity on fluid flow through a single fracture," *Water Resources Research*, 29(9): 1209-15, (1984).

United States Environmental Protection Agency (US EPA). "The state-of-the practice of characterization and remediation of contaminated ground water at fractured rock sites." EPA 542-R-01-010. Washington D.C., July 2001.

United States Environmental Protection Agency (US EPA). "Contaminant Transport in Fractured Media: Models for Decision Makers." EPA/540/4-89/004. Washington D.C., June 2002.

United States Environmental Protection Agency (US EPA). "Technical Factsheet on Trichloroethylene." http://www.epa.gov/OGWDW/dwh/t-voc/trichlor.html. 20 May 2004.

United States Geological Survey (USGS). "Fractured Rock Aquifers: Understanding an Increasingly Important Source of Water." http://toxics.usgs.gov/pubs/FS-112-02/fs-112-02.pdf. 25 July 2004.

Vandergraaf, T.T. "Radionuclide migration experiments under laboratory conditions," *Geophysical Research Letters*, 22(11): 1409-12 (1995).

Way, S.S. and C.R. McKee. "Restoration of in-situ coal gasification sites from naturally occurring flow and dispersion," *In Situ*, 5: 77-101 (1981).

Wealthall, Gary P., David N. Lerner, and Steven F. Thornton. "Predicting NAPL Source Zones in Fractured Rock," *NATO/CCMS Pilot Project on Contaminated Land and Groundwater (Phase III)*. EPA 542-R-02-011. Washington D.C., January 2003.

Wellman, Tristan and Eileen Poeter. "Software Review – FracMan," International Ground Water Modeling Center Newsletter, 21: 5 (Spring 2003).

Wilson, C.R. and P.A. Witherspoon. "Flow interference effects at fracture intersections," *Water Resources Research*, 12: 102-104 (1976).

Witherspoon, P.A., J.S.Y. Wang, K. Iwai, and J.E. Gale. "Validity of cubic law for fluid flow in a deformable rock fracture," *Water Resources Research*, 16(6): 1016-1024 (1980).

Witherspoon, P.A., J.C.S. Long, E.L. Majer, and L.R. Myer. "A new seismic-hydraulic approach to modeling flow in fractured rocks." Proceedings, NWWA/IGWMC Conference on solving ground water problems with models, Denver, CO, Feb 1987.

Wu, Yu-Shu, H.H. Liu, and G.S. Bodvarsson. "Effect of small-scale fractures on flow and transport processes at Yucca Mountain, Nevada," *Lawrence Berkeley National Laboratory,* Paper LBNL-51848 (December 5, 2002).

Wu, Y.S., H.H. Liu, and G.S. Bodvarsson. "A triple-continuum approach for modeling flow and transport processes in fractured rock," *Journal of Contaminant Hydrology*, 73: 145-179 (2004).

Vita

Captain Jason M. Bordas graduated from Stuttgart American High School in Pattonville, Germany. He entered undergraduate studies at the University of Cincinnati where he graduated with a Bachelor of Science degree in Civil Engineering in June 1997. He was commissioned through Officer Training School in Maxwell AFB.

His first assignment was at Dyess AFB as Chief of Contract Management for the 7th Civil Engineer Squadron. While Stationed at Dyess, he deployed overseas in August 2000 to spend four months in Riyadh, Saudi Arabia as Chief of Maintenance Engineering for the 320th Expeditionary Civil Engineer Squadron. In August 2001, he was assigned to the 39th Civil Engineer Squadron, Incirlik AB, Turkey where he served as Expeditionary Operations Flight Chief. In August 2003, he entered the Graduate School of Engineering and Management, Air Force Institute of Technology. Upon graduation, he will be assigned to HQ AFMC/CE.

REPORT DOCUMENTATION PAGE

Form Approved
OMB No. 074-0188

1. REPORT DATE *(DD-MM-YYYY)*	**2. REPORT TYPE**	**3. DATES COVERED** *(From – To)*
21-03-2005	**Master's Thesis**	Sep 2003 – Mar 2005

4. TITLE AND SUBTITLE

Modeling Groundwater Flow and Contaminant Transport in Fractured Aquifers

5a. CONTRACT NUMBER

5b. GRANT NUMBER

5c. PROGRAM ELEMENT NUMBER

6. AUTHOR(S)

Bordas, Jason M., Captain, USAF

5d. PROJECT NUMBER

5e. TASK NUMBER

5f. WORK UNIT NUMBER

7. PERFORMING ORGANIZATION NAMES(S) AND ADDRESS(S)

Air Force Institute of Technology
Graduate School of Engineering and Management (AFIT/EN)
2950 Hobson Way
WPAFB OH 45433-7765

8. PERFORMING ORGANIZATION REPORT NUMBER

AFIT/GEM/ENV/05M-02

9. SPONSORING/MONITORING AGENCY NAME(S) AND ADDRESS(ES)

Lt Col Mark H. Smith
AFCEE/TD
3300 Sidney Brooks
Brooks City-Base TX 78235 DSN 240-3332 Mark.H.Smith@brooks.af.mil

10. SPONSOR/MONITOR'S ACRONYM(S)

11. SPONSOR/MONITOR'S REPORT NUMBER(S)

12. DISTRIBUTION/AVAILABILITY STATEMENT

APPROVED FOR PUBLIC RELEASE; DISTRIBUTION UNLIMITED.

13. SUPPLEMENTARY NOTES

14. ABSTRACT

The hybrid discrete fracture network/equivalent porous medium (DFN/EPM) model was selected for analysis and application to simulate a contaminated site in this study. The DFN/EPM was selected because it appeared to have the potential to aid decision making by remedial project managers at contaminated DoD fractured aquifer sites. This model can use data that are typically available at a site while incorporating the important processes relevant to describing contaminant transport in a fractured medium. The model was applied to simulate the operation of a pump-and-treat remedial action at a trichloroethene-contaminated fractured aquifer at Pease AFB. The model was able to simulate the salient characteristics of hydraulic and contaminant data collected at the site during operation of the remediation pump-and-treat system. The model was then used to evaluate the impact of various pump-and-treat system designs on contaminant containment at the site. Based on these model simulations, the potential benefits to site managers of using the DFN/EPM approach to model groundwater flow and contaminant transport at fractured aquifer sites were demonstrated.

15. SUBJECT TERMS

Groundwater contamination, Pease AFB, fractured media, equivalent porous media, discrete fracture network, groundwater modeling

16. SECURITY CLASSIFICATION OF:			**17. LIMITATION OF ABSTRACT**	**18. NUMBER OF PAGES**	**19a. NAME OF RESPONSIBLE PERSON**
REPORT	**ABSTRACT**	**c. THIS PAGE**			Prof Mark N. Goltz, ENV
U	**U**	**U**	**UU**	119	**19b. TELEPHONE NUMBER** *(Include area code)* (937) 255-3636, ext 4638; e-mail: Mark.Goltz@afit.edu

Standard Form 298 (Rev: 8-98)
Prescribed by ANSI Std. Z39-18